

# **Supporting Information**

## **Synthesis and Structural Characterization of Anion Complexes with Azacalix[2]dipyrrolylmethane: Effect of Anion Charge on the Conformation of the Macrocycle**

Tapas Guchhait,<sup>a</sup> Ganesan Mani,<sup>\*,a</sup> and Carola Schulzke<sup>b</sup>

<sup>a</sup>Department of Chemistry, Indian Institute of Technology Kharagpur, Kharagpur, India 721 302

<sup>b</sup>Institut für Biochemie, Ernst-Moritz-Arndt Universität Greifswald, Felix-Hausdorff-Straße 4, D-17487 Greifswald, Germany. E-mail: [carola.schulzke@uni-greifswald.de](mailto:carola.schulzke@uni-greifswald.de)

\*Corresponding Author: [gmani@chem.iitkgp.ernet.in](mailto:gmani@chem.iitkgp.ernet.in)

## NMR and IR spectra

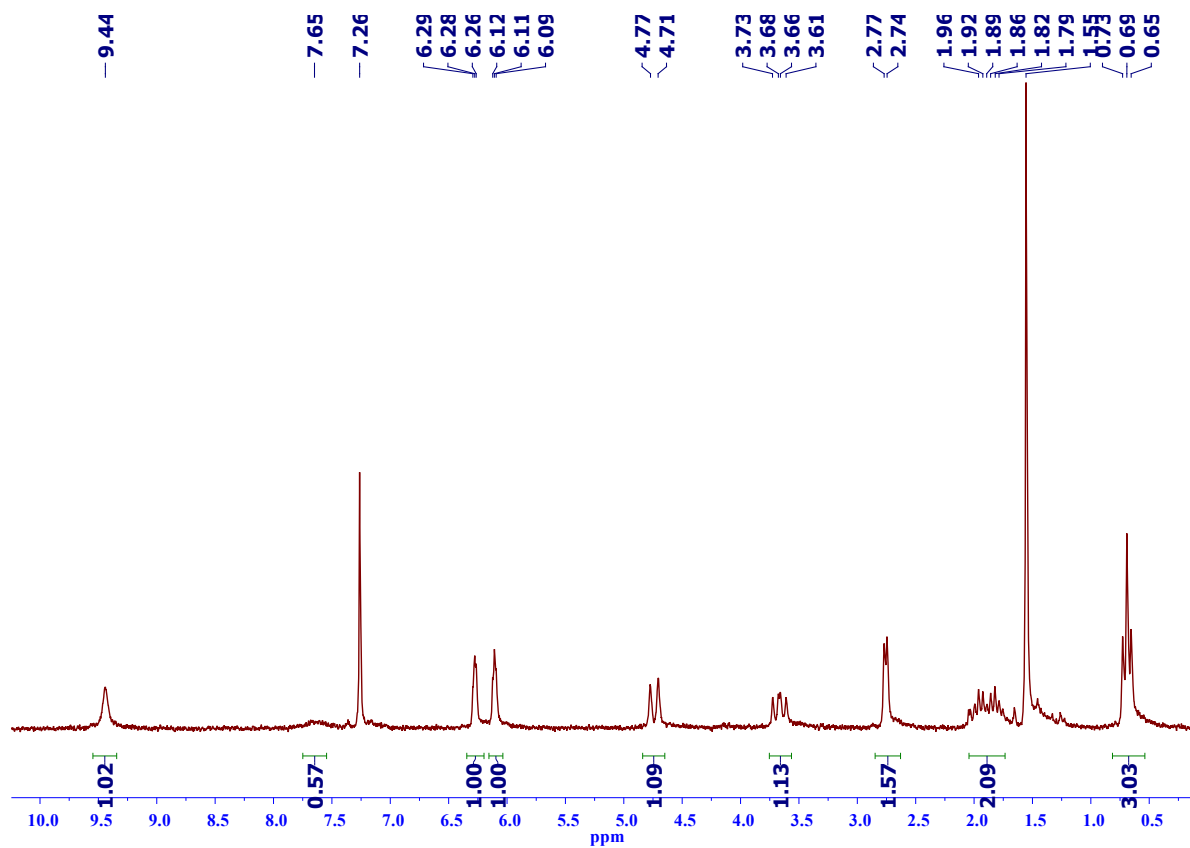


**Figure S1.** <sup>1</sup>H NMR (200 MHz) spectrum of the nitrate complex, **2a** in CDCl<sub>3</sub> at room temperature.

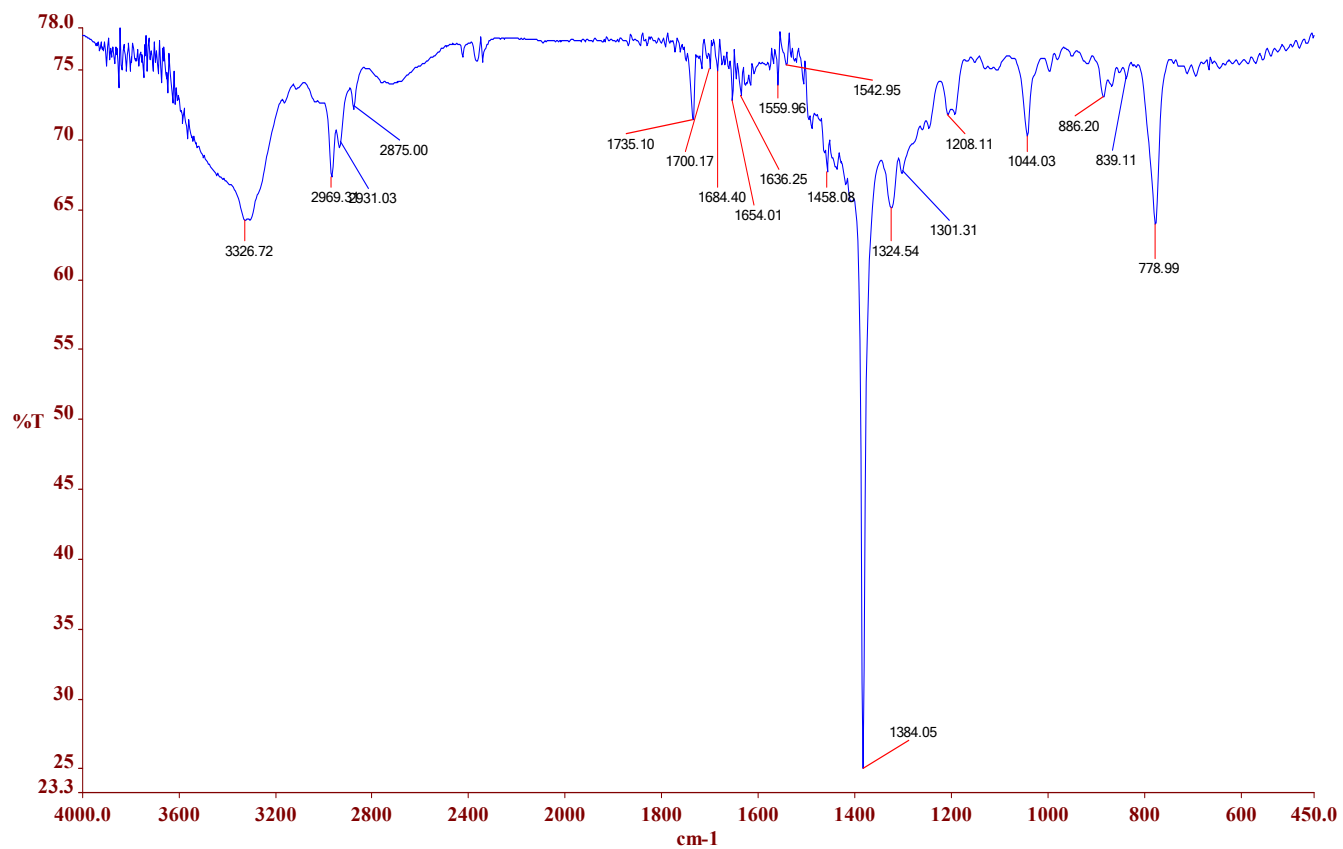


**Figure S2.** IR spectrum of the nitrate complex, **2a** recorded as a KBr disc.

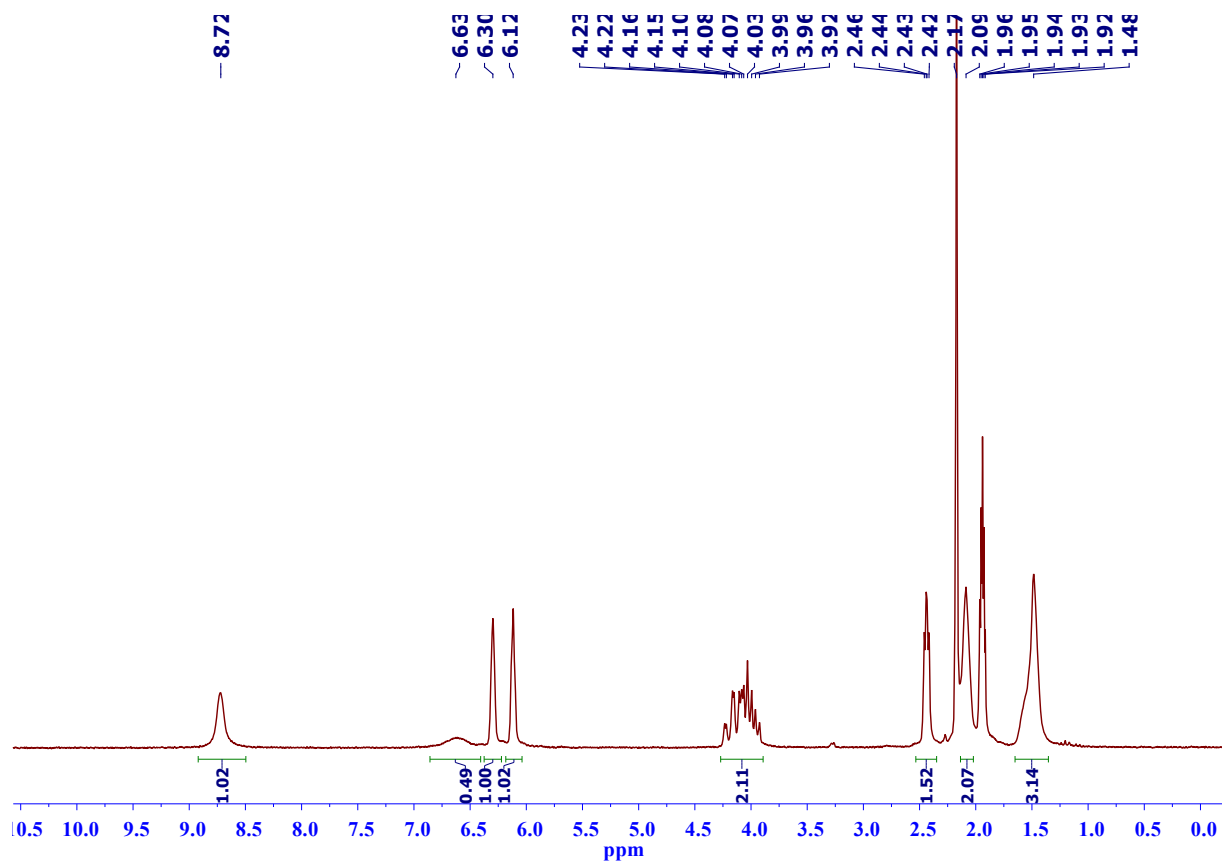


**Figure S3.** <sup>1</sup>H NMR (200 MHz) spectrum of the tetrafluoroborate complex, **2b** in CD<sub>3</sub>CN at room temperature.

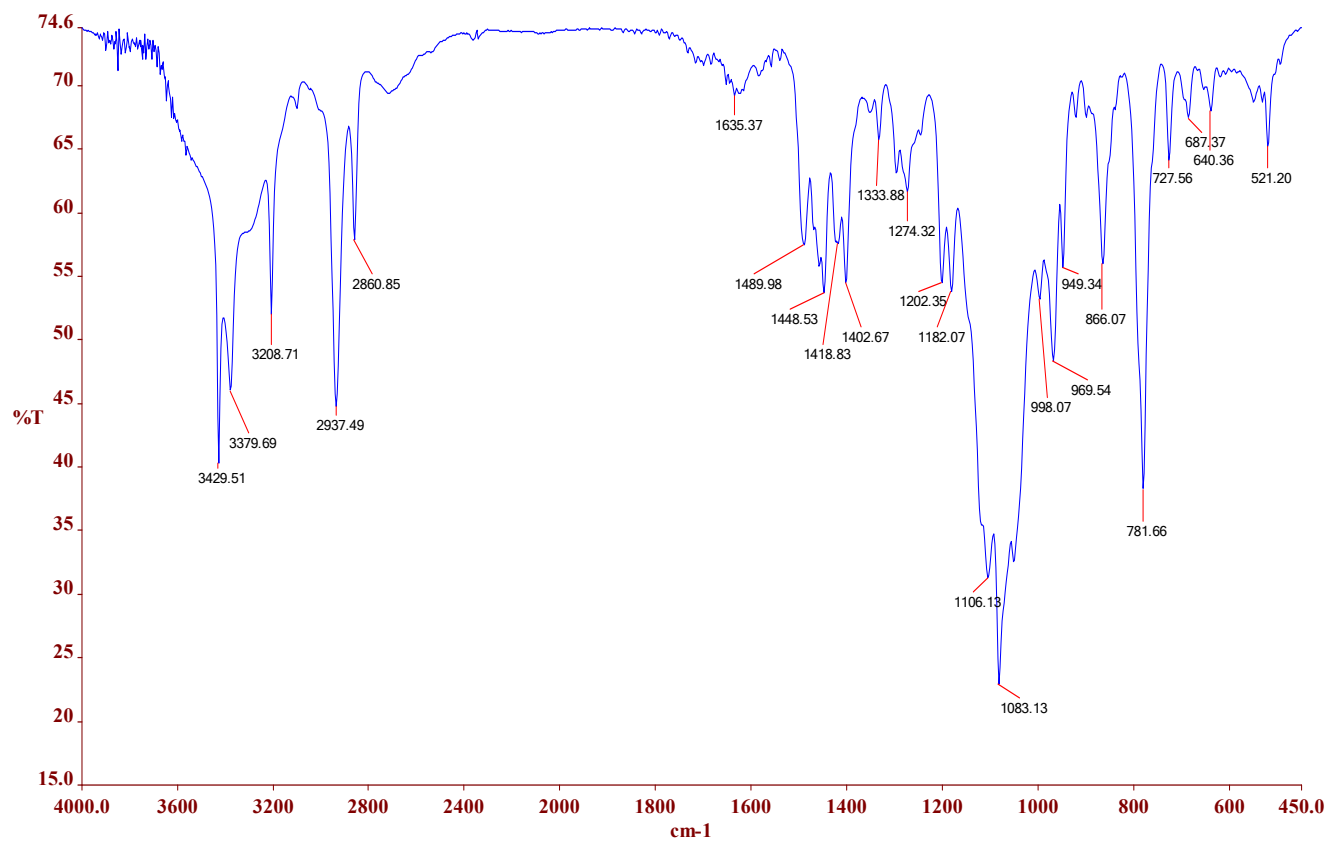


**Figure S4.** IR spectrum of the tetrafluoroborate complex, **2b** recorded as a KBr disc.

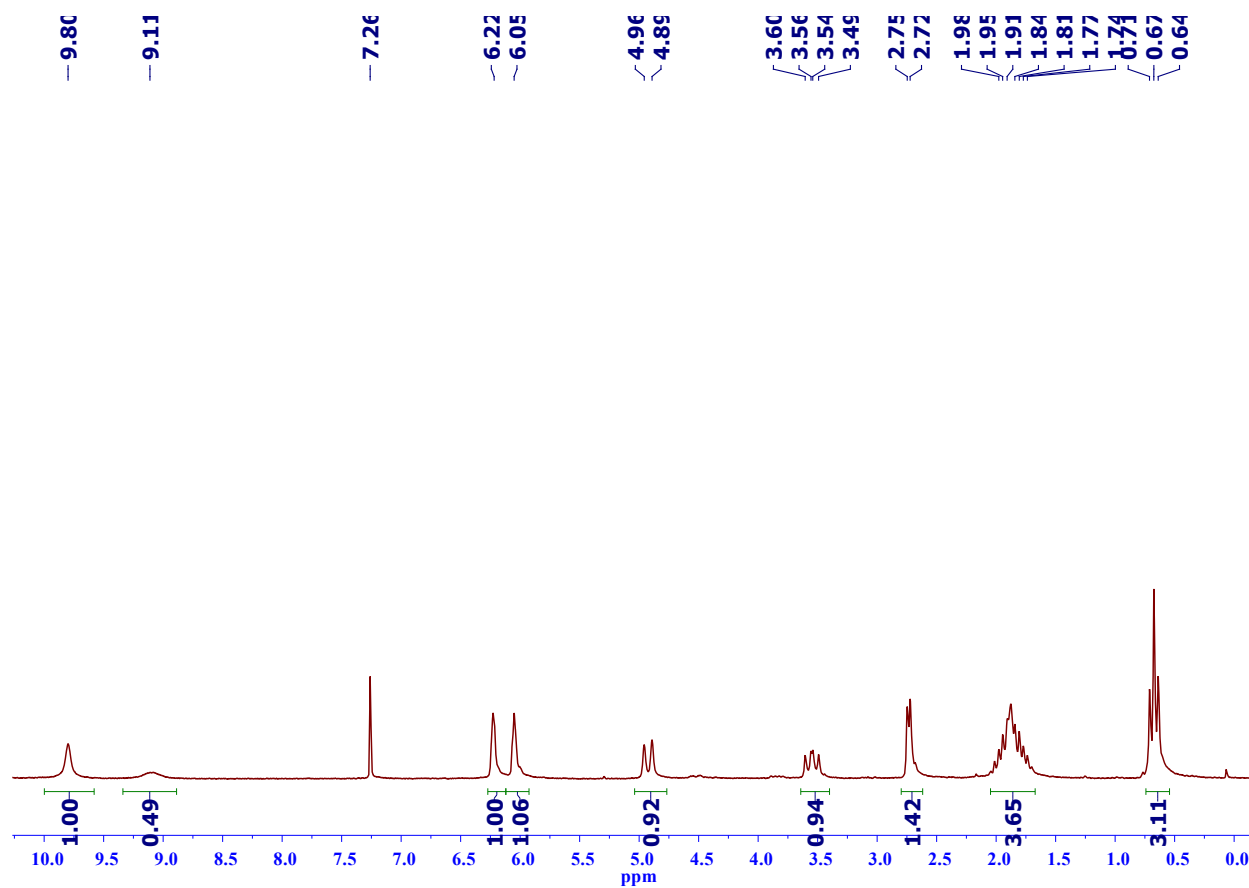


**Figure S5.**  $^1\text{H}$  NMR (200 MHz) spectrum of the chloride complex, **2c** in  $\text{CDCl}_3$  at room temperature.

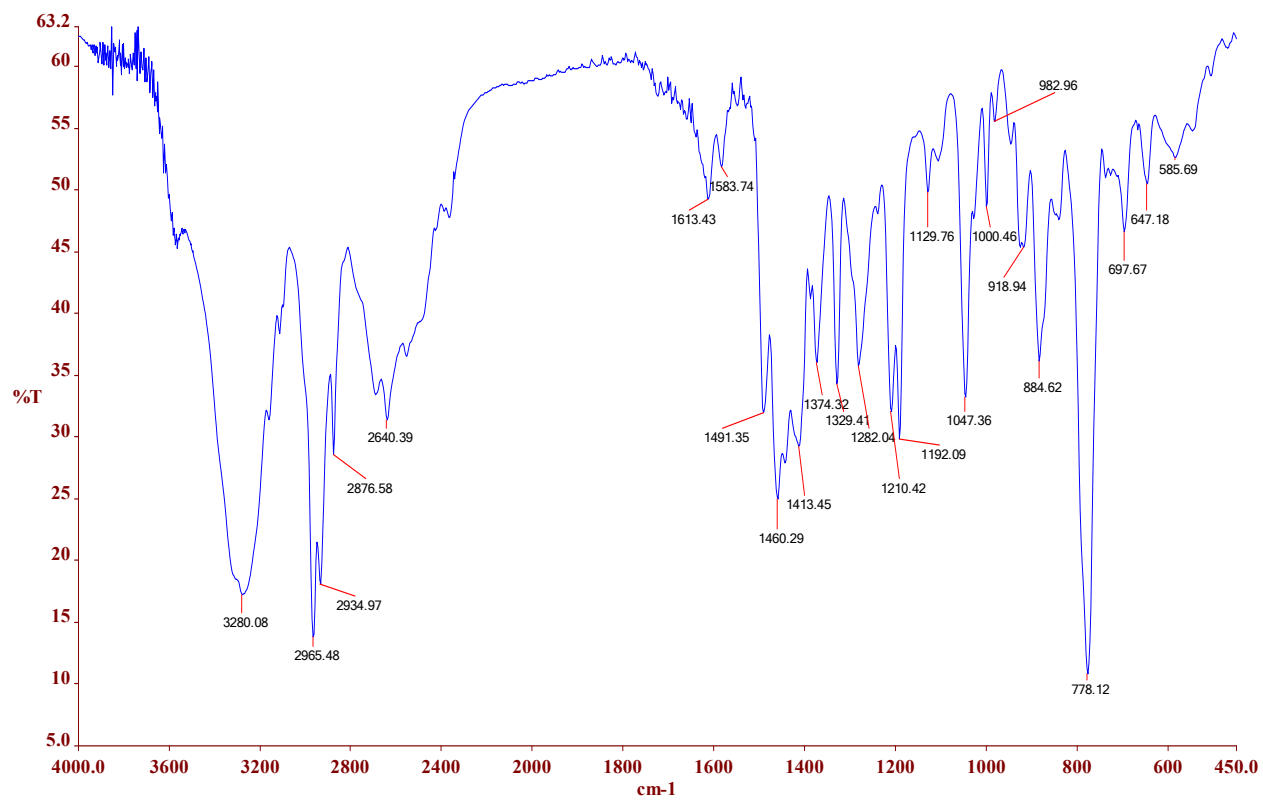


**Figure S6.** IR spectrum of the chloride complex, **2c** recorded as a KBr disc.

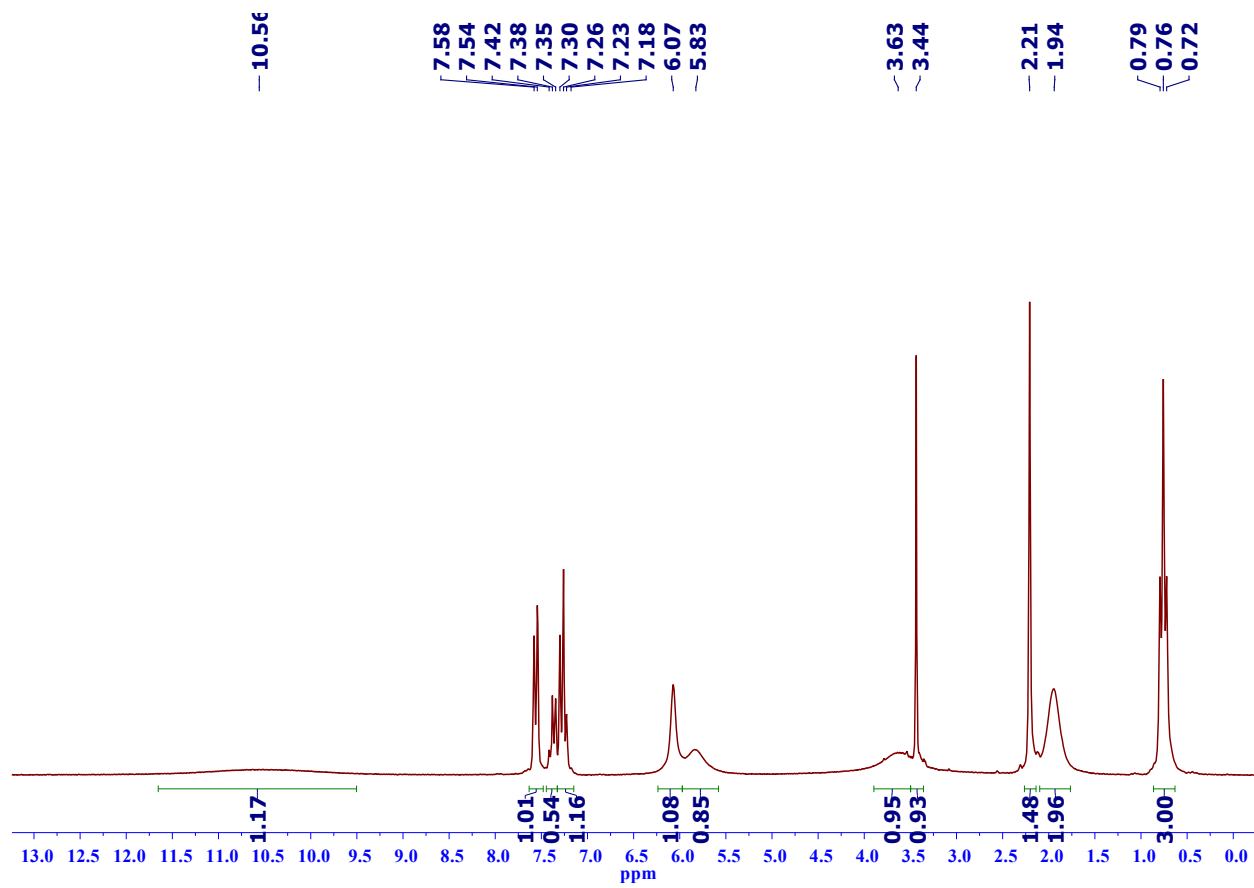


**Figure S7.**  $^1\text{H}$  NMR (200 MHz) spectrum of the benzoate complex, **2d** in  $\text{CDCl}_3$  at room temperature.

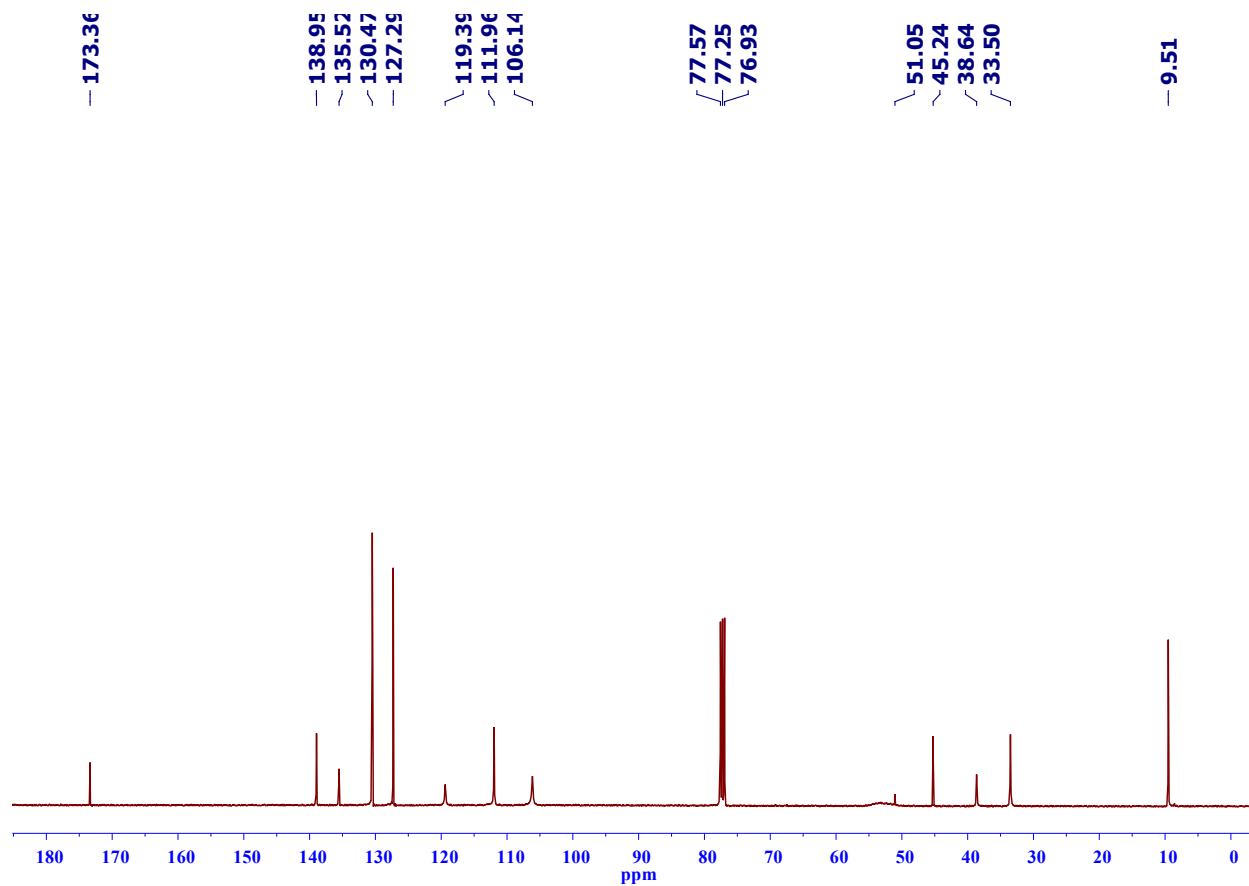


**Figure S8.**  $^{13}\text{C}\{^1\text{H}\}$  NMR (100.6 MHz) spectrum of the benzoate complex, **2d** in  $\text{CDCl}_3$  at room temperature.

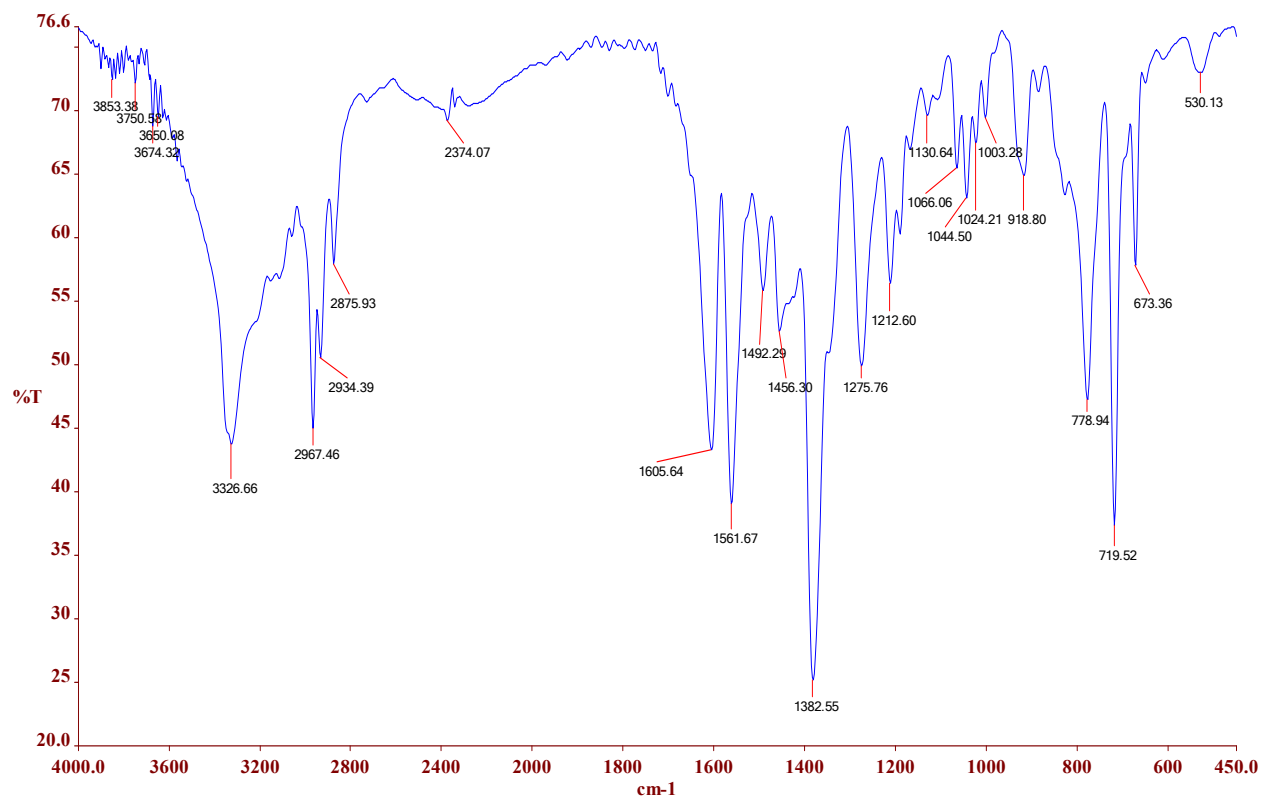


**Figure S9.** IR spectrum of the benzoate complex, **2d** recorded as a KBr disc.

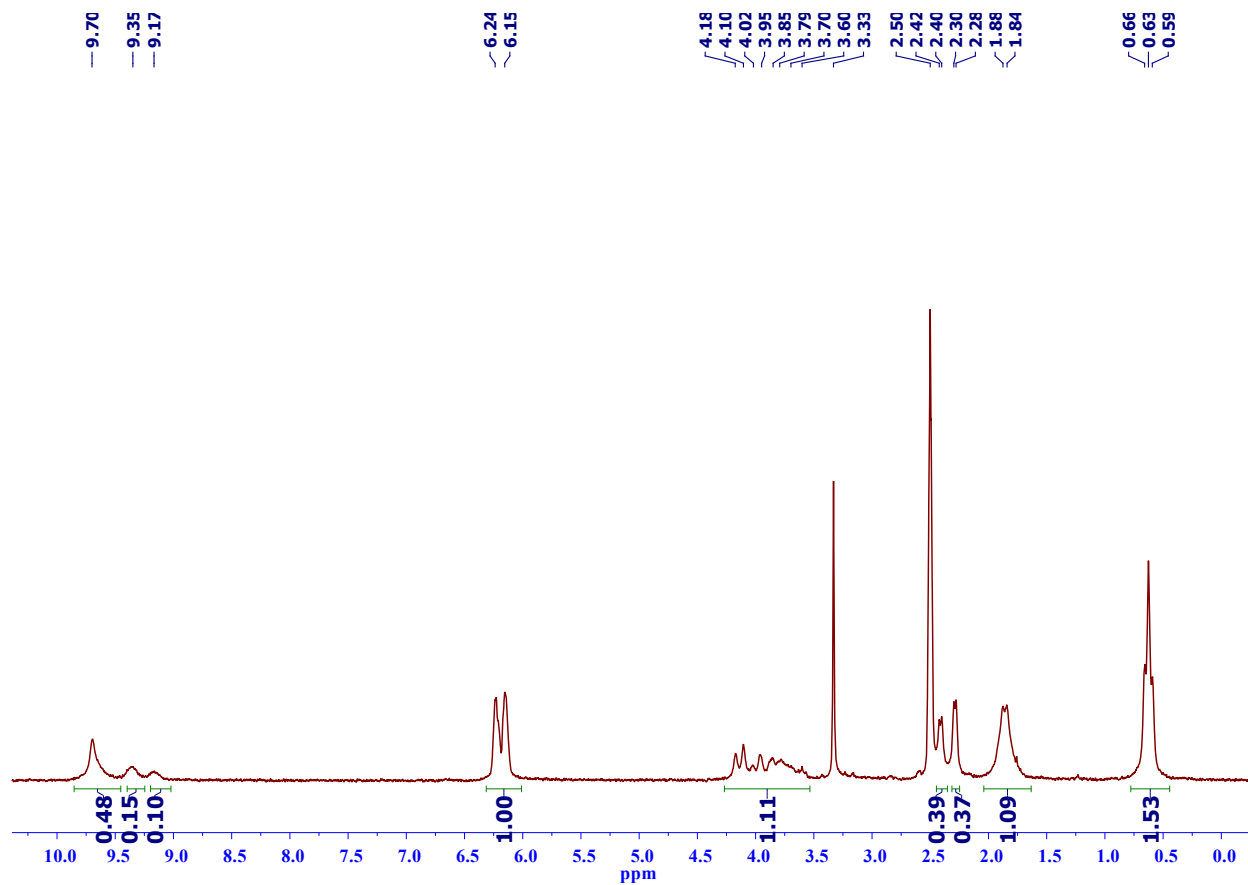


**Figure S10.** <sup>1</sup>H NMR (200 MHz) spectrum of the perchlorate complex, **2e** in DMSO-*d*<sub>6</sub> at room temperature.

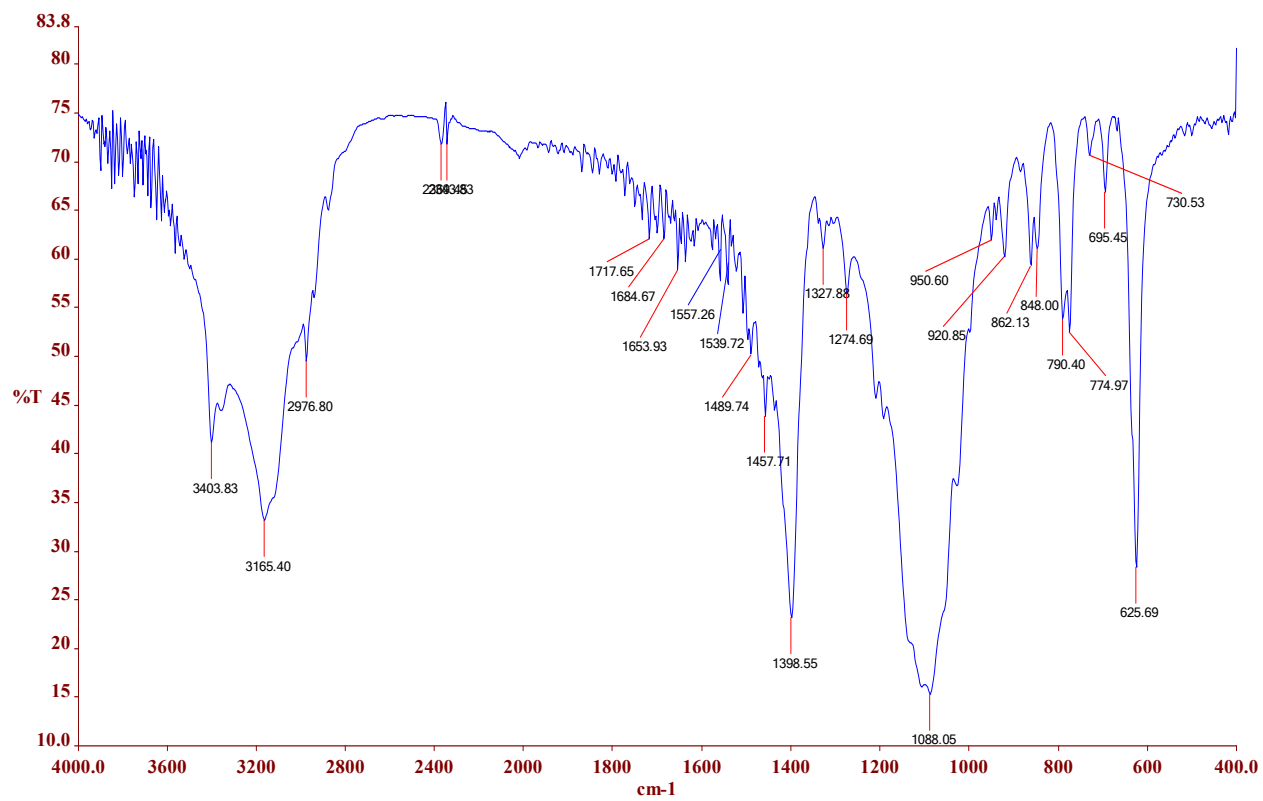


**Figure S11.** IR spectrum of the perchlorate complex, **2e** recorded as a KBr disc.

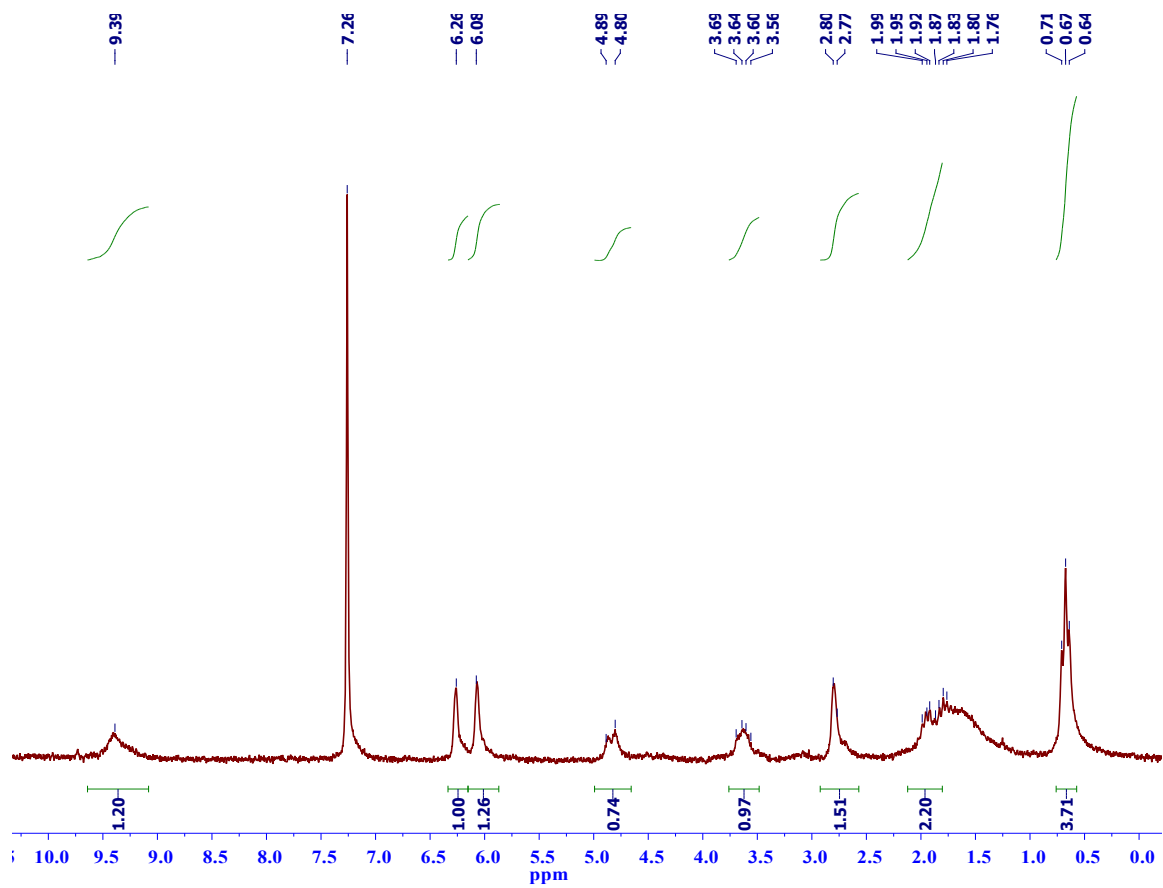


**Figure S12.**  $^1\text{H}$  NMR (200 MHz) spectrum of the chromate complex, **2f** recorded in  $\text{CDCl}_3$  at room temperature.

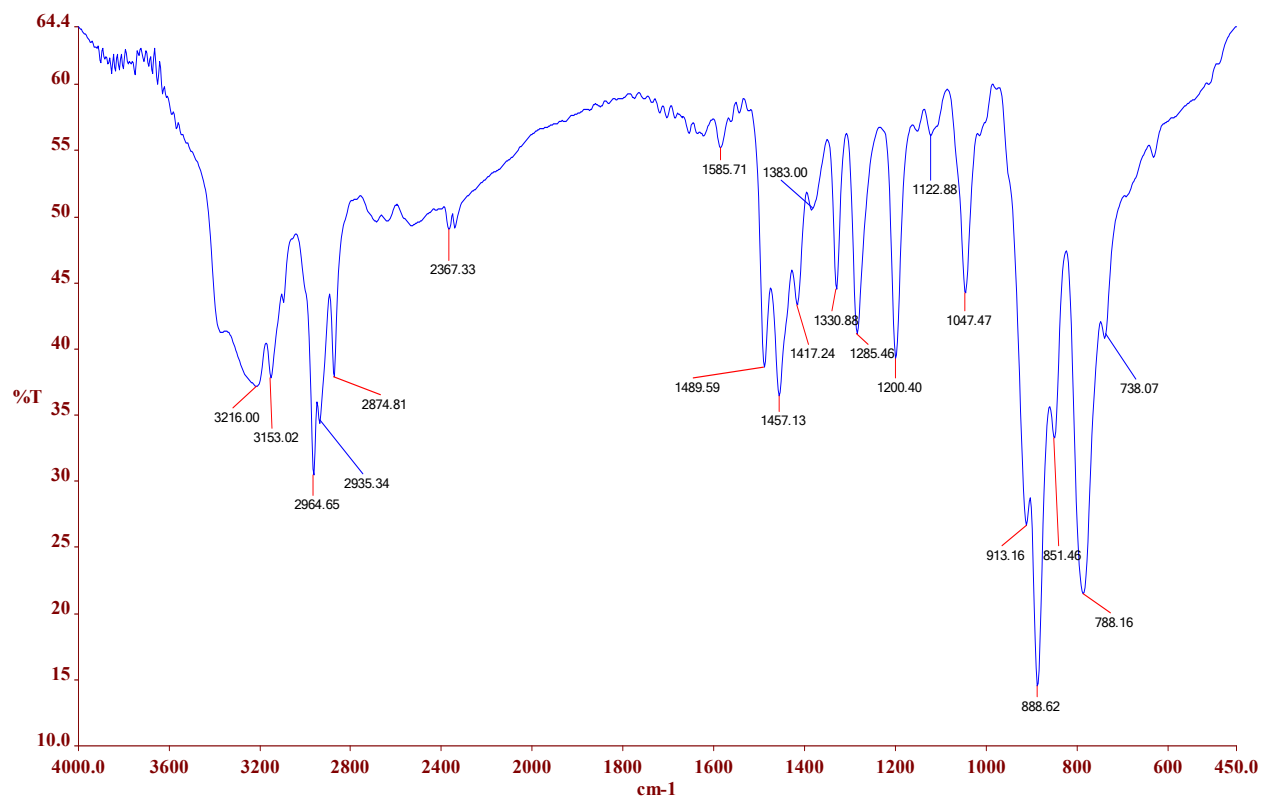


**Figure S13.** IR spectrum of the chromate complex, **2f** recorded as a KBr disc.

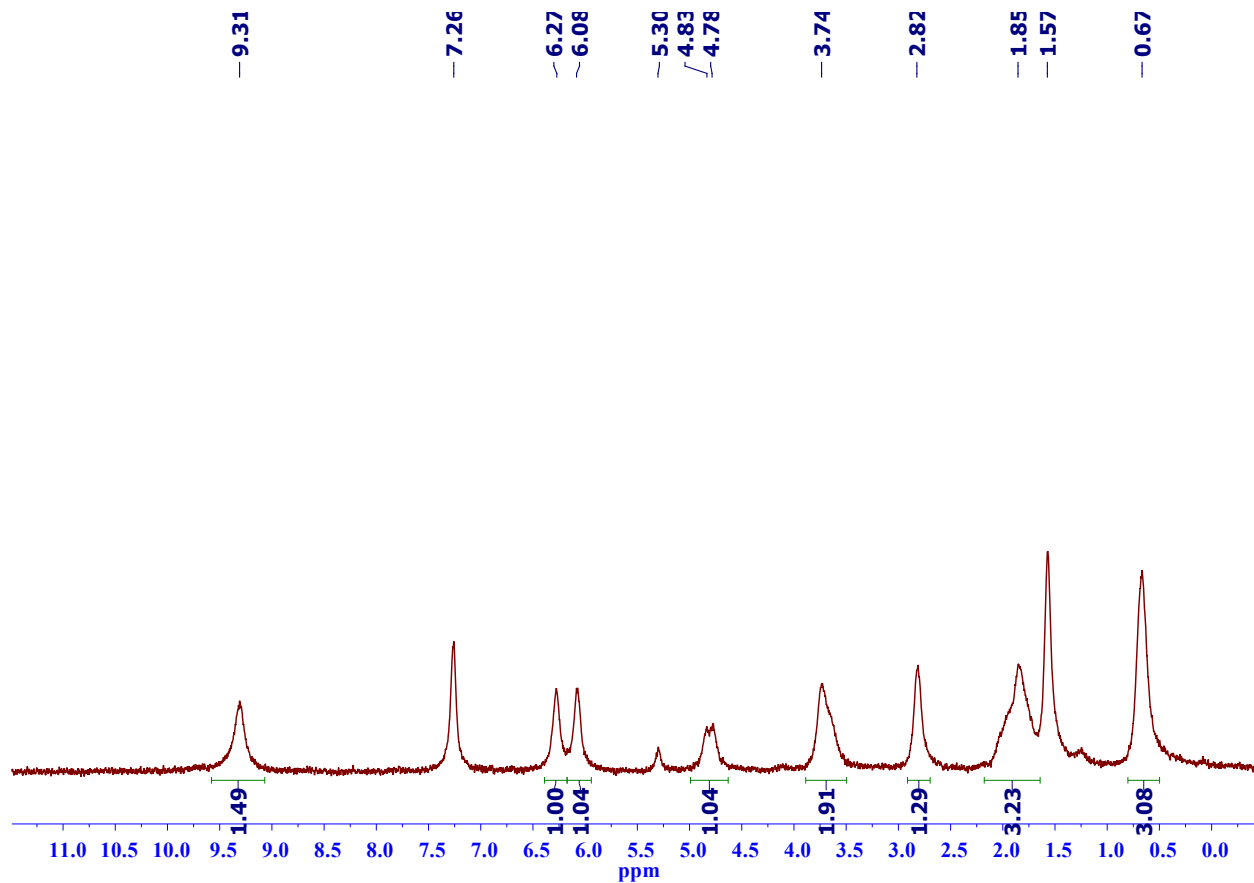


**Figure S14.** <sup>1</sup>H NMR (200 MHz) spectrum of the dichromate complex, **2g** recorded in CDCl<sub>3</sub> at room temperature.

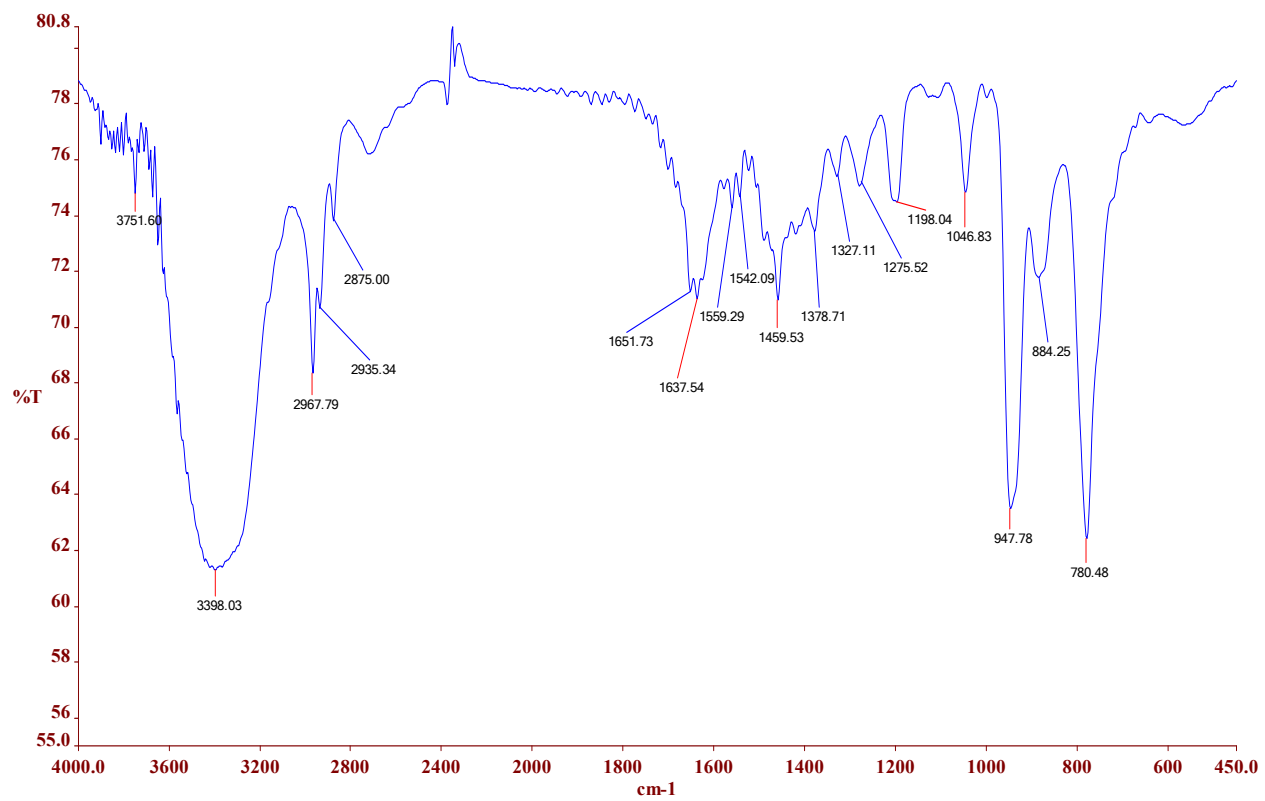


**Figure S15.** IR spectrum of the dichromate complex, **2g** recorded as a KBr disc.

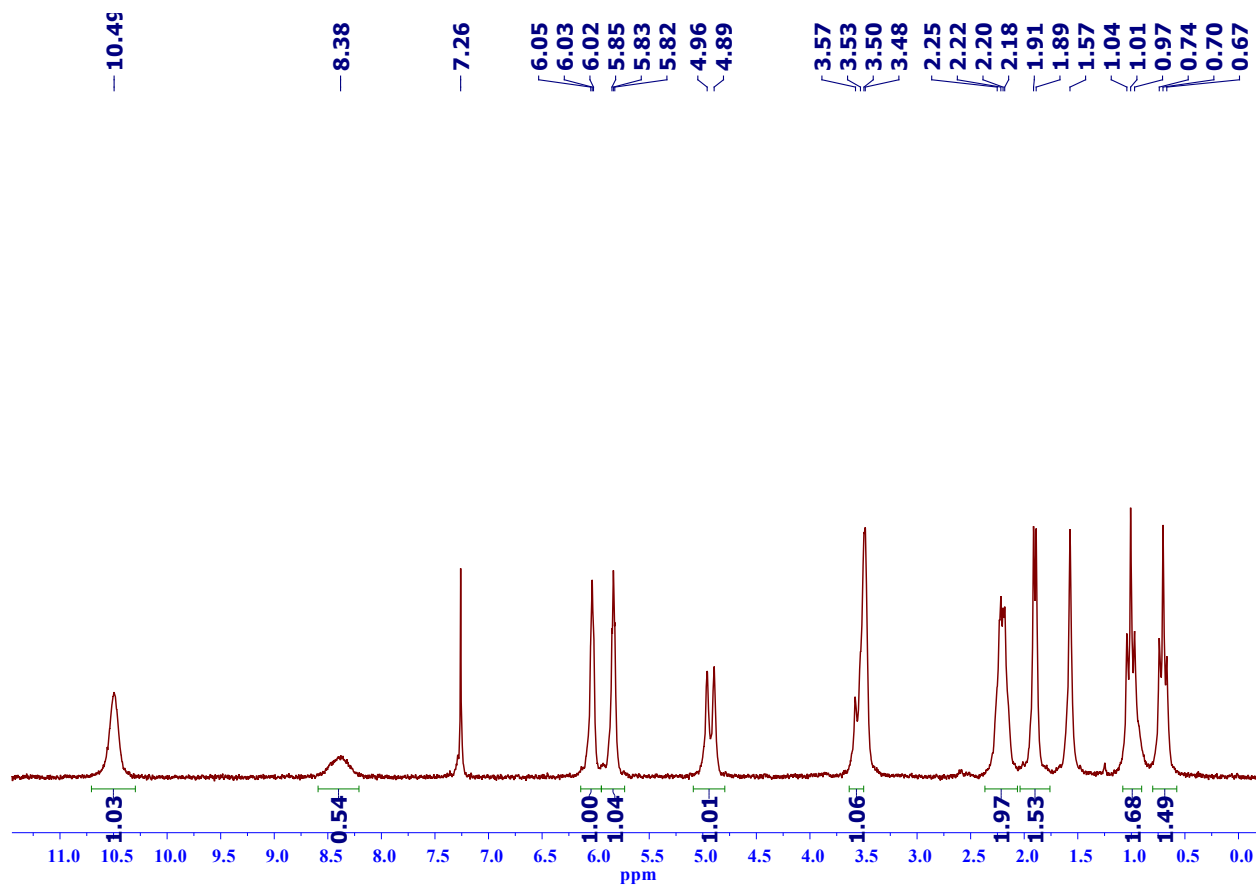


**Figure S16.** <sup>1</sup>H NMR (200 MHz) spectrum of the hexafluorosilicate complex, **2h** in CDCl<sub>3</sub> at room temperature.

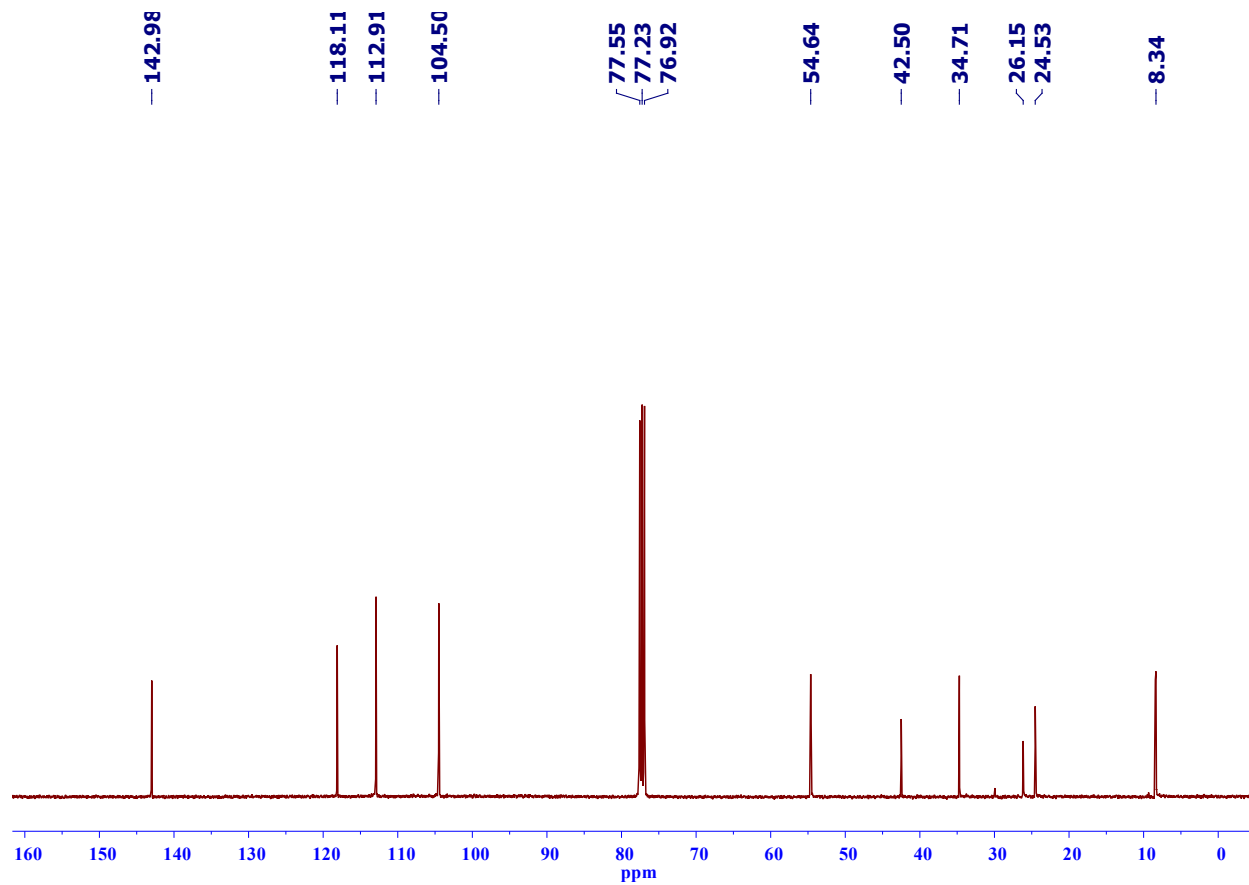


**Figure S17.**  $^{13}\text{C}\{^1\text{H}\}$  NMR (100.6 MHz) spectrum of the hexafluorosilicate complex, **2h** in  $\text{CDCl}_3$  at room temperature.

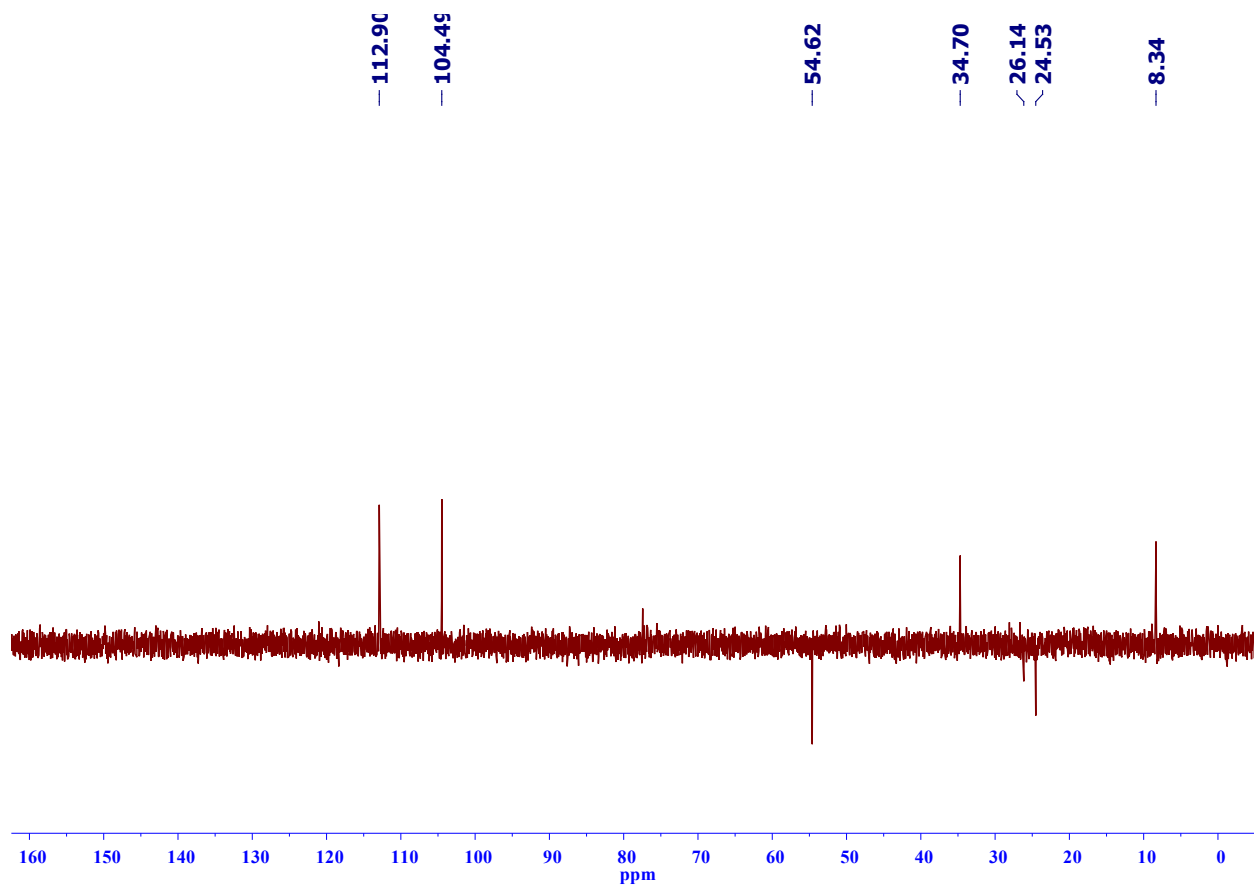


**Figure S18.** DEPT-135 $\{^1\text{H}\}$  NMR (100.6 MHz) spectrum of the hexafluorosilicate complex, **2h** in  $\text{CDCl}_3$  at room temperature.

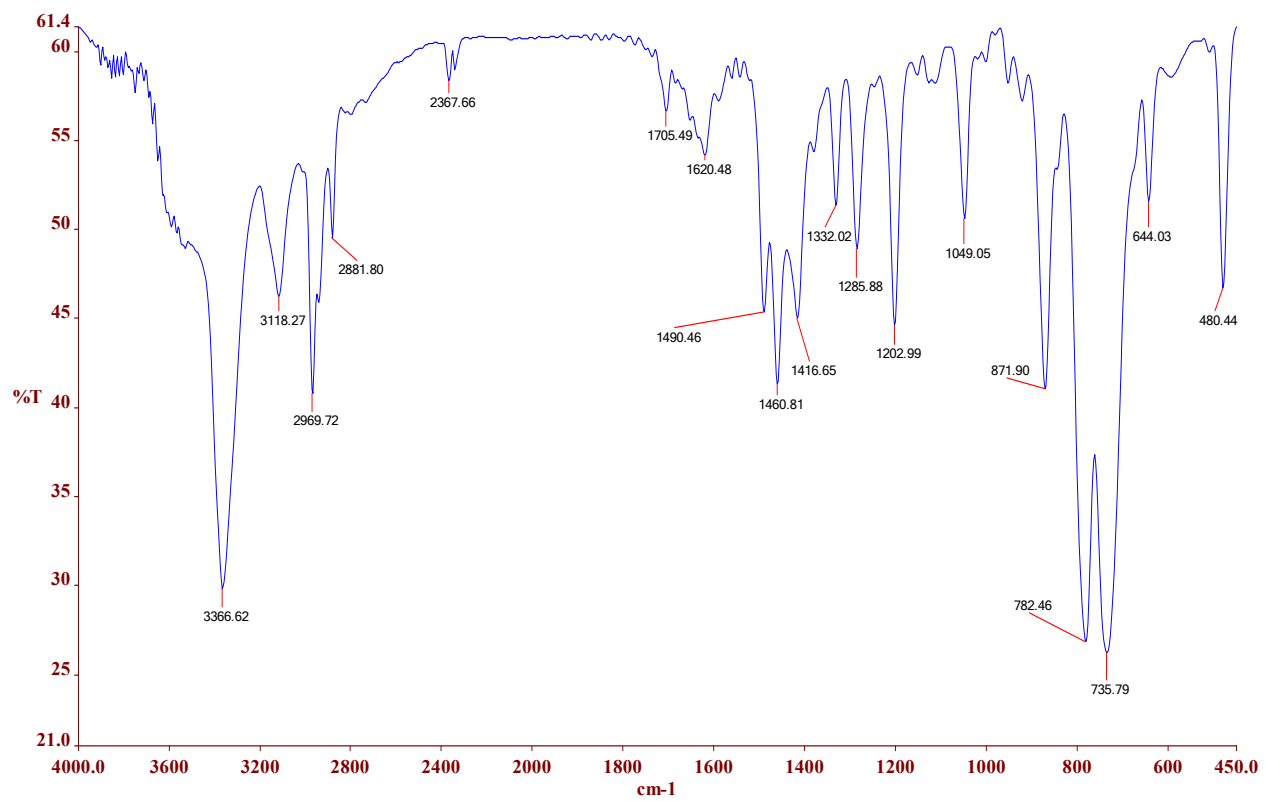


**Figure S19.** IR spectrum of hexafluorosilicate complex, **2h** recorded as a KBr disc.

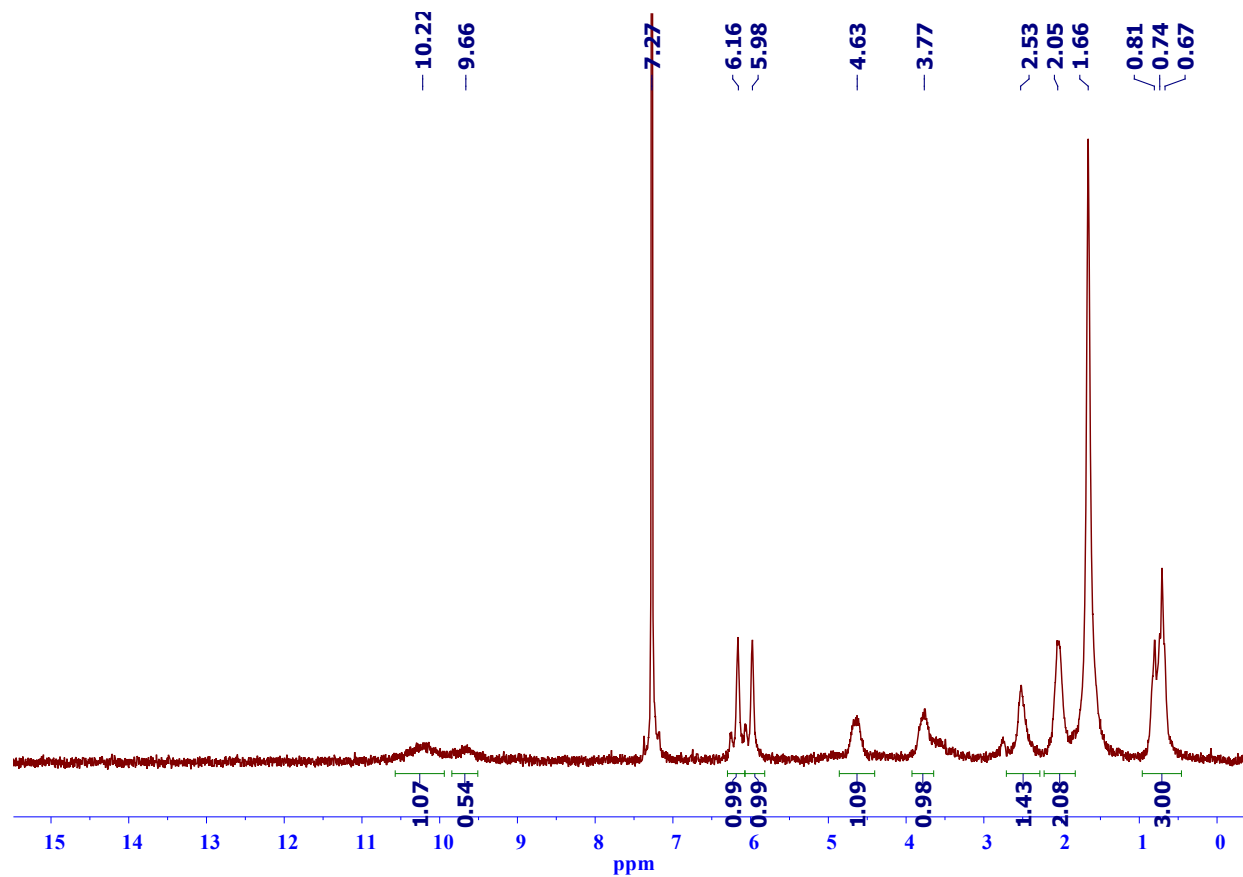


**Figure S20.** <sup>1</sup>H NMR (200 MHz) spectrum of the thiosulfate complex, **2i** in CDCl<sub>3</sub> at room temperature.

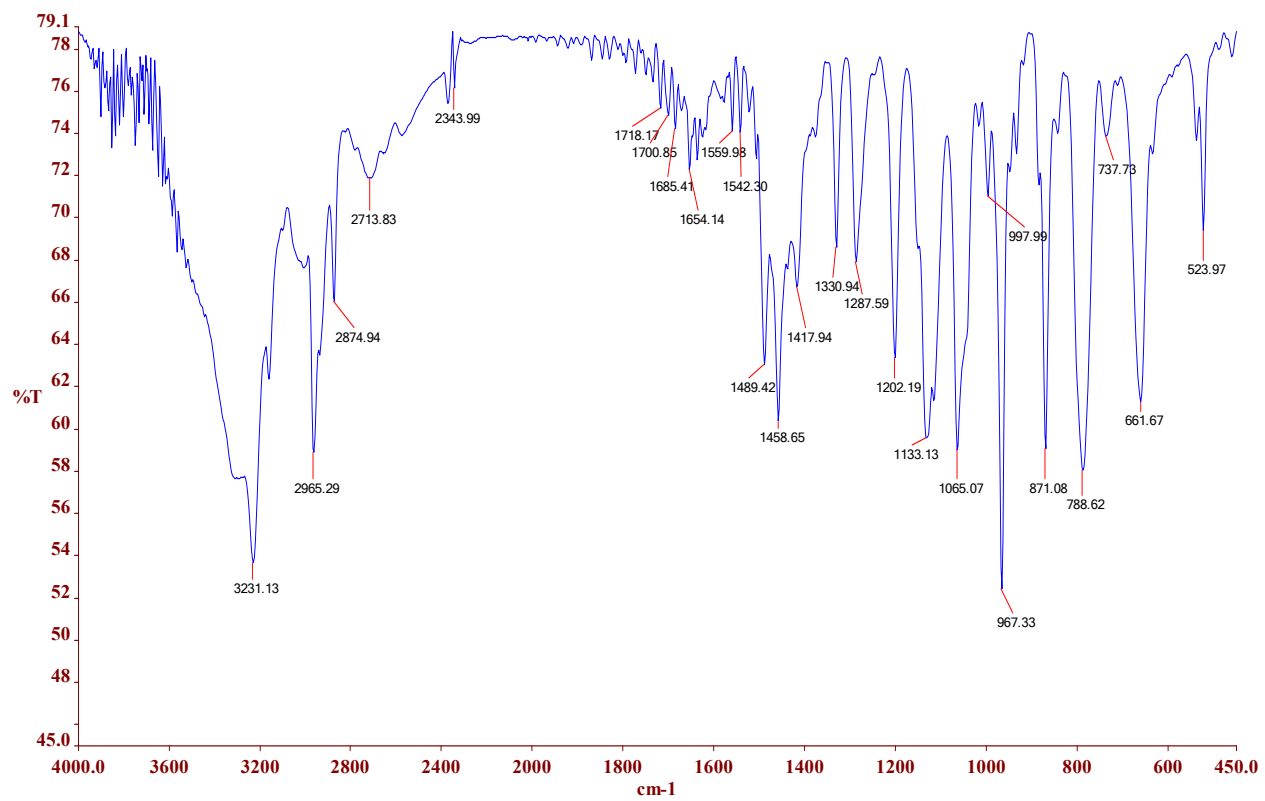


**Figure S21.** IR spectrum of the thiosulfate complex, **2i** recorded as a KBr disc.

## X-ray structures

### Special refinement details

For **2a** two disorders were found, one at the nitrate for which one oxygen atom (O2; 63% vs. 37% occupancy) is split over two locations and one at the co-crystallized ethylacetate of which one carbon (C33; 71% vs. 29% occupancy) is split over two locations. Both disorders were modeled with constrained parameters (SADI/SIMU/DELU).

All hydrogen atoms on the nitrogen atoms were located and refined freely with respect to location but the  $U_{iso}$  values were constrained to  $1.2 U_{eq}$  of their pivot atoms.

For **2b** the  $\text{BF}_4^-$  ion is disordered affecting three out of the four F atoms (F2-F4) which are all split over two positions (as a rotation around the B1-F1 axis) with occupations of 73% (major) vs. 27% (minor). No constraints or restraints were used except constraining the F1 – F(X) distances (SADI). All N-bound hydrogen atoms were located and refined freely without any constraints or restraints.

For **2c** three of the dangling ethyl groups appear to be not as well behaved as the rest of the molecule. Modelling the respective disorder did not improve the overall quality of the refinement. Therefore only some constraints (SIMU/DELU) were applied to the respective atoms (C1, C2, C18, C19, C20, C21). All N-bound hydrogen atoms were located and refined freely with respect to location. The  $U_{iso}$  values of these hydrogen atoms were constrained within two groups (aromatic vs. amine functions) using free variables.

For **2d** the co-crystallized methanol solvent is completely disordered over two positions (C47, O5; 73% vs 27% occupancy). In addition one ethyl substituent is disordered over two positions (C25, C26; 84% vs. 16% occupancy). Both disorders were modeled with constrained parameters (SADI - only for –Et/SIMU/DELU). One of the respective already split carbon atoms is still showing signs of disorder plus there is also some “movement” in other ethyl substituents and one phenyl ring of the guest molecule, none of which could be modelled properly, i.e. no improvement of the refinement was achieved. Therefore it was decided to rather accept large ADP max/min ratios for the respective atoms than to almost completely fix their refinement parameters in order to get a stable refinement. All N-bound hydrogen atoms were located and refined freely with respect to location. The  $U_{iso}$  values of these hydrogen atoms were constrained within two groups (aromatic vs. amine functions) using free variables. Overall the crystal was diffracting only very weakly in addition to the substantial disorder and consequently the obtained data are limited. However, the data which were gathered are quite consistent with a very low  $R_{int}$  value. We are therefore confident that the refined structure is an appropriate reflection of the actual situation in the crystalline solid state.

For **2e** all eight oxygen atoms of the two  $\text{ClO}_4^-$  guest ions are disordered with the tetrahedral ions tumbling around the central chlorine atoms. The occupancies are 60% vs. 40% around Cl1 and 56% vs 44% around Cl2. The respective fractions of the atoms look as if they might want to be split even further indicating that the ions do behave almost like isotropic spheres only restricted

in their movement by the hydrogen bonds with the macrocycle. The disordered oxygen atoms were constrained using SAME, SIMU and DELU. All N-bound hydrogen atoms were located and refined without any restraints or constraints.

For **2f** the N-H distances for N1, N2, N3 and N4 were constrained (SADI) and the  $U_{iso}$  values of the respective hydrogen atoms were constrained to  $1.2 U_{eq}$  of their pivot atoms. Two methyl (C17, C18) groups of two ethyl substituents on the same carbon are disordered over two positions each (both with occupancies of ca. 55% vs. 45%). The disorder was modelled using constraints (SIMU/DELU). The guest ion chromate  $\text{CrO}_4^{2-}$  is disordered by a rotation around the Cr-O1 axis. The respective fractions were set to 50%. SIMU and DELU constraints were used.

For **2g** the N-bound hydrogen atoms at N1, N3, N4, N5 and N6 were located, the respective N-H distances were constrained (SADI) and the  $U_{iso}$  values of the respective hydrogen atoms were constrained to  $1.2 U_{eq}$  of their pivot atoms. The hydrogen atom on tetrahedral N2 was placed using the riding model for a methine proton.

The dichromate guest ion is disordered over two positions concerning all atoms (both Cr and seven O). The refinement of all these atoms was constrained (SAME/SIMU/DELU). The occupancies of the two positions are 83% vs. 17%.

The crystal lattice contains quite large solvent accessible voids and residual electron density which could not be refined. The SQUEEZE/PLATON procedure yielded total void volume and electron count of  $920.0 \text{ \AA}^3$  and  $360 e^-$ . It was concluded that nine molecules water are present per formula which could not be refined. These routines necessarily contribute to the discrepancy between calculated and reported formulae in the cif-file. The solvent has been treated as a diffuse contribution to the overall scattering without specific atom positions.

The obtained hkl file was truncated due to the severe disorder (dichromate and nine water molecules) in order to avoid accounting for predominantly noise.

For **2h** the three N-bound hydrogen atoms (the whole macrocycle is generated by symmetry operation) were located and refined freely with respect to location but the  $U_{iso}$  values of the respective hydrogen atoms were constrained to  $1.2 U_{eq}$  of their pivot atoms for aromatic and to  $1.5 U_{eq}$  for tetrahedral pivot atoms. The guest ion  $\text{SiF}_6^{2-}$  ion is disordered over two positions by a ca.  $45^\circ$  rotation about the F1-Si1-F2 axis. The occupancies are 86% vs. 16%. The disorder was modeled using constraints (SADI for the Si-F distances/SIMU/DELU). Per formula two methanol molecules co-crystallized, which were not refineable and were treated with the SQUEEZE/PLATON procedure yielding total void volume and electron count of  $648 \text{ \AA}^3$  and  $168 e^-$ , respectively. These routines necessarily contribute to the discrepancy between calculated and reported formulae in the cif-file. The solvent has been treated as a diffuse contribution to the overall scattering without specific atom positions.

For **2i** all N-bound hydrogen atoms were located and their positions first constrained using SADI for the N-H distances but this resulted in rather long N-H distances of  $1.01 \text{ \AA}$  and many short H-H distances in the structure. Consequently the N-H distances were restrained to the typical value (DFIX 0.87 0.05). The hydrogen atom's  $U_{iso}$  values were constrained to  $1.2 U_{eq}$  of their pivot atoms. All ethyl substituents (C23 C24 C25 C26 C28 C29 C30 C31) of the macrocycle are disordered over two positions each with the major occupancies ranging from 51% to 54%. The

thiosulfate anion is disordered over two positions involving all atoms of the ion. The occupancies are 83% vs. 17%. Two oxygen atoms of minor occupancy were refined isotropically. For all atoms of this disordered molecule constraints were used (SAME/SIMU/DELU).

**Table 1** Crystallographic data for **2a**, **2b**, **2c**, **2d** and **2e**.

	<b>2a·EtOAc</b>	<b>2b</b>	<b>2c·CH<sub>3</sub>OH</b>	<b>2d·0.5MeOH</b>	<b>2e</b>
Empirical formula	C <sub>36</sub> H <sub>56</sub> N <sub>8</sub> O <sub>8</sub>	C <sub>34</sub> H <sub>48</sub> B <sub>2</sub> F <sub>8</sub> N <sub>6</sub>	C <sub>33</sub> H <sub>52</sub> Cl <sub>2</sub> N <sub>6</sub> O	C <sub>47</sub> H <sub>62</sub> N <sub>6</sub> O <sub>5</sub>	C <sub>32</sub> H <sub>48</sub> Cl <sub>2</sub> N <sub>6</sub> O <sub>8</sub>
Formula weight	728.88	714.40	619.70	791.02	715.66
Wavelength (Å)	0.71073	0.71073	0.71073	0.71073	0.71073
Temperature (K)	298(2)	298(2)	298(2)	298(2)	298(2)
Crystal system	Triclinic	Monoclinic	Triclinic	Triclinic	Triclinic
Color and shape	Colorless, prism	Colorless, prism	Colorless, prism	Colorless, prism	Colorless, prism
Space group	<i>P</i> -1	<i>P</i> 2 <sub>1</sub> / <i>c</i>	<i>P</i> -1	<i>P</i> -1	<i>P</i> -1
<i>a</i> /Å	11.231(2)	11.3232(9)	11.4134(14)	12.8015(8)	10.826(5)
<i>b</i> /Å	13.224(3)	12.4132(10)	11.7294(14)	13.1729(8)	10.886(5)
<i>c</i> /Å	13.496(3)	12.8292(10)	14.5809(17)	14.8039(8)	15.397(7)
<i>α</i> /degree	86.976(6)	90.0	101.215(4)	72.028(3)	86.377(13)
<i>β</i> /degree	88.508(6)	98.879(2)	109.626(4)	87.892(3)	81.065(14)
<i>γ</i> /degree	85.740(6)	90.0	96.150(4)	70.142(3)	81.984(12)
Volume (Å <sup>3</sup> )	1995.6(7)	1781.6(2)	1771.8(4)	2227.0(2)	1773.4(13)
<i>Z</i>	2	2	2	2	2
<i>D</i> <sub>calcd</sub> , g cm <sup>-3</sup>	1.213	1.332	1.162	1.180	1.340
<i>μ</i> /mm <sup>-1</sup>	0.087	0.108	0.217	0.077	0.240
<i>F</i> (000)	784	752	668	852	760
<i>θ</i> range (degree)	1.511 to 31.444	1.820 to 31.789	1.530 to 24.171	1.450 to 20.608	1.340 to 24.663
Limiting indices	-16<= <i>h</i> <=15, -18<= <i>k</i> <=15, -17<= <i>l</i> <=19	-16<= <i>h</i> <=15, -17<= <i>k</i> <=18, -18<= <i>l</i> <=18	-12<= <i>h</i> <=13, -13<= <i>k</i> <=13, -16<= <i>l</i> <=15	-12<= <i>h</i> <=12, -12<= <i>k</i> <=13, -14<= <i>l</i> <=14	-12<= <i>h</i> <=12, -12<= <i>k</i> <=12, -18<= <i>l</i> <=18
Total/ unique no. of reflns.	29256 / 10905	25832 / 5614	19156 / 5590	15300 / 4471	20498 / 5963
<i>R</i> <sub>int</sub>	0.1229	0.0700	0.0640	0.0327	0.0451
Data / restr. / params.	10905 / 42 / 514	5614 / 15 / 267	5590 / 21 / 406	4471 / 94 / 592	5963 / 120 / 537
GOF ( <i>F</i> <sup>2</sup> )	0.942	1.013	0.887	1.039	1.019
<i>R</i> <sub>1</sub> , <i>wR</i> <sub>2</sub>	0.0872, 0.1637	0.0762, 0.1578	0.0700, 0.2015	0.0472, 0.1155	0.0476, 0.1071
R indices (all data)					
<i>R</i> <sub>1</sub> , <i>wR</i> <sub>2</sub>	0.3297, 0.2528	0.1914, 0.2011	0.1341, 0.2357	0.0665, 0.1310	0.0823, 0.1262
Largest different peak and hole (e Å <sup>-3</sup> )	0.419 and -0.296	0.401 and -0.222	0.561 and -0.266	0.455 and -0.216	0.296 and -0.244

**Table 2** Crystallographic data for **2f**, **2g**, **2h** and **2i**.

	<b>2f</b>	<b>2g·9H<sub>2</sub>O</b>	<b>2h·2MeOH</b>	<b>2i</b>
--	-----------	---------------------------	-----------------	-----------

Empirical formula	C <sub>32</sub> H <sub>46</sub> CrN <sub>6</sub> O <sub>4</sub>	C <sub>32</sub> H <sub>66</sub> Cr <sub>2</sub> N <sub>6</sub> O <sub>16</sub>	C <sub>34</sub> H <sub>56</sub> F <sub>6</sub> N <sub>6</sub> O <sub>2</sub> Si	C <sub>32</sub> H <sub>48</sub> N <sub>6</sub> O <sub>3</sub> S <sub>2</sub>
Formula weight	630.75	894.90	722.93	628.88
Wavelength (Å)	1.54178	1.54178	0.71073	1.54178
Temperature (K)	110(2)	110(2)	293(2)	293(2)
Crystal system	Orthorhombic	Monoclinic	Monoclinic	Monoclinic
Color and shape	yellow, needle	orange, needle	Colorless, prism	Colorless, needle
Space group	<i>Cmc2(1)</i>	<i>P2<sub>1</sub>/n</i>	<i>C2/c</i>	<i>P2<sub>1</sub></i>
<i>a</i> /Å	17.1257(9)	8.815(3)	12.93(2)	11.660(9)
<i>b</i> /Å	16.2367(9)	17.954(6)	10.616(16)	11.998(9)
<i>c</i> /Å	11.2669(6)	26.463(9)	27.70(4)	11.826(9)
$\alpha$ /degree	90.0	90.0	90.0	90.0
$\beta$ /degree	90.0	96.493(11)	99.20(3)	92.19(2)
$\gamma$ /degree	90.0	90.0	90.0	90.0
Volume (Å <sup>3</sup> )	3132.9(3)	4162(2)	3753(10)	1653(2)
<i>Z</i>	4	4	4	2
<i>D</i> <sub>calcd</sub> , g cm <sup>-3</sup>	1.337	1.428	1.280	1.263
$\mu$ /mm <sup>-1</sup>	3.378	4.943	0.131	1.790
<i>F</i> (000)	1344	1904	1544	676
$\theta$ range (degree)	3.751 to 59.969	2.980 to 59.983	1.489 to 27.345	3.794 to 59.999
Limiting indices	-19 $\leq$ h $\leq$ 19, -18 $\leq$ k $\leq$ 18, -12 $\leq$ l $\leq$ 12	-9 $\leq$ h $\leq$ 9, -20 $\leq$ k $\leq$ 20, -29 $\leq$ l $\leq$ 29	-16 $\leq$ h $\leq$ 16, -13 $\leq$ k $\leq$ 13, -34 $\leq$ l $\leq$ 33	-11 $\leq$ h $\leq$ 13, -13 $\leq$ k $\leq$ 13, -13 $\leq$ l $\leq$ 13
Total/ unique no. of reflns.	33664 / 2405	27489 / 5821	14408 / 3904	12097 / 4602
<i>R</i> <sub>int</sub>	0.0845	0.1608	0.1183	0.1222
Data / restr./ params.	2405/ 19 / 252	5821 / 234 / 476	3904 / 24 / 235	4602 / 288 / 519
GOF ( <i>F</i> <sup>2</sup> )	1.013	0.916	0.877	0.834
<i>RI</i> , <i>wR2</i>	0.0449, 0.1091	0.0760, 0.1535	0.0689, 0.1391	0.0695, 0.1437
R indices (all data) <i>RI</i> , <i>wR2</i>	0.0530, 0.1114	0.1435, 0.1791	0.1744, 0.1690	0.1264, 0.1602
Largest different peak and hole (e Å <sup>-3</sup> )	0.212 and -0.436	0.412 and -0.317	0.227 and -0.202	0.224 and -0.233

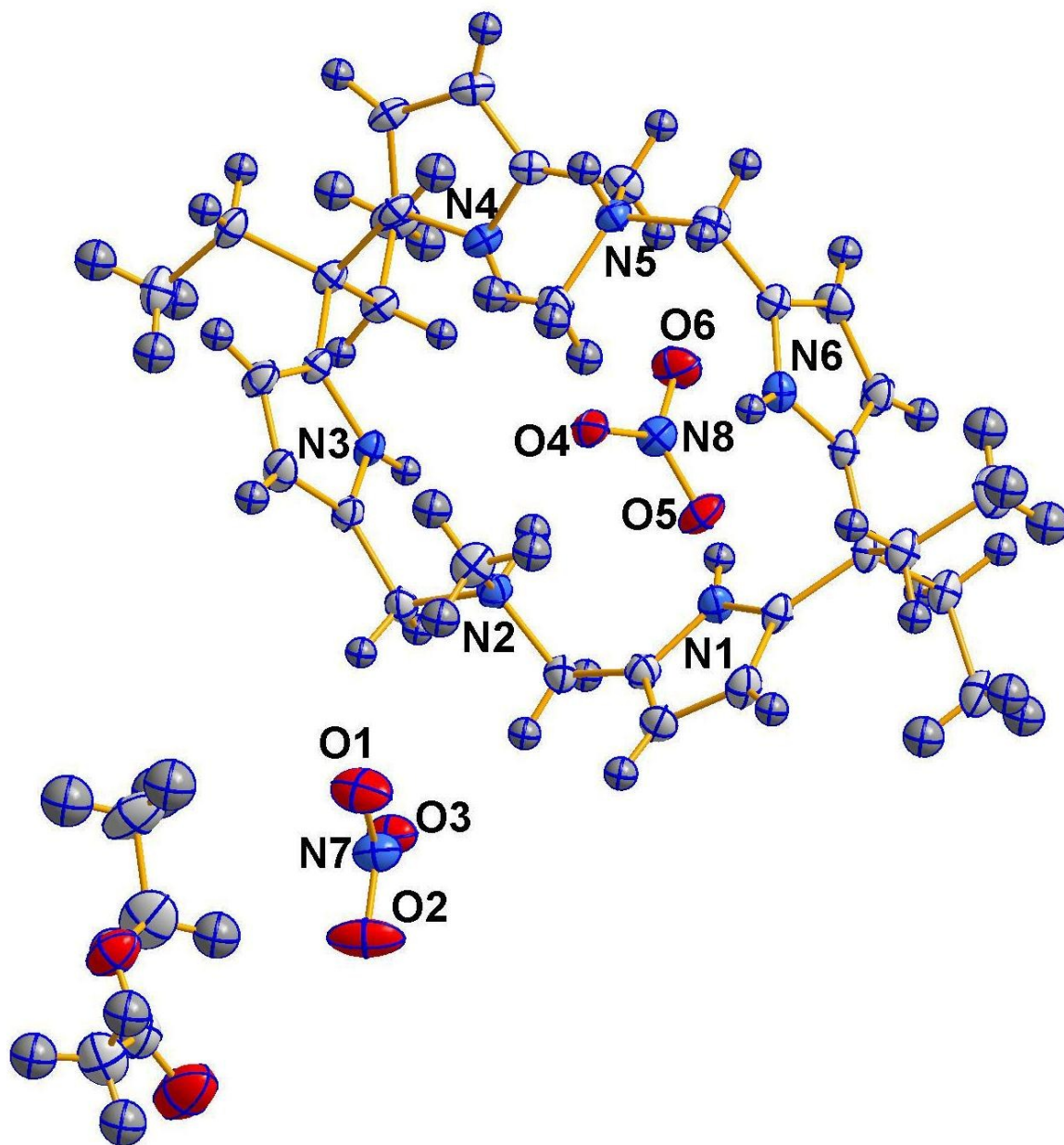


**Figure S22.** ORTEP diagram of the nitrate ion complex **2a**, showing the asymmetric unit (50% thermal ellipsoids).

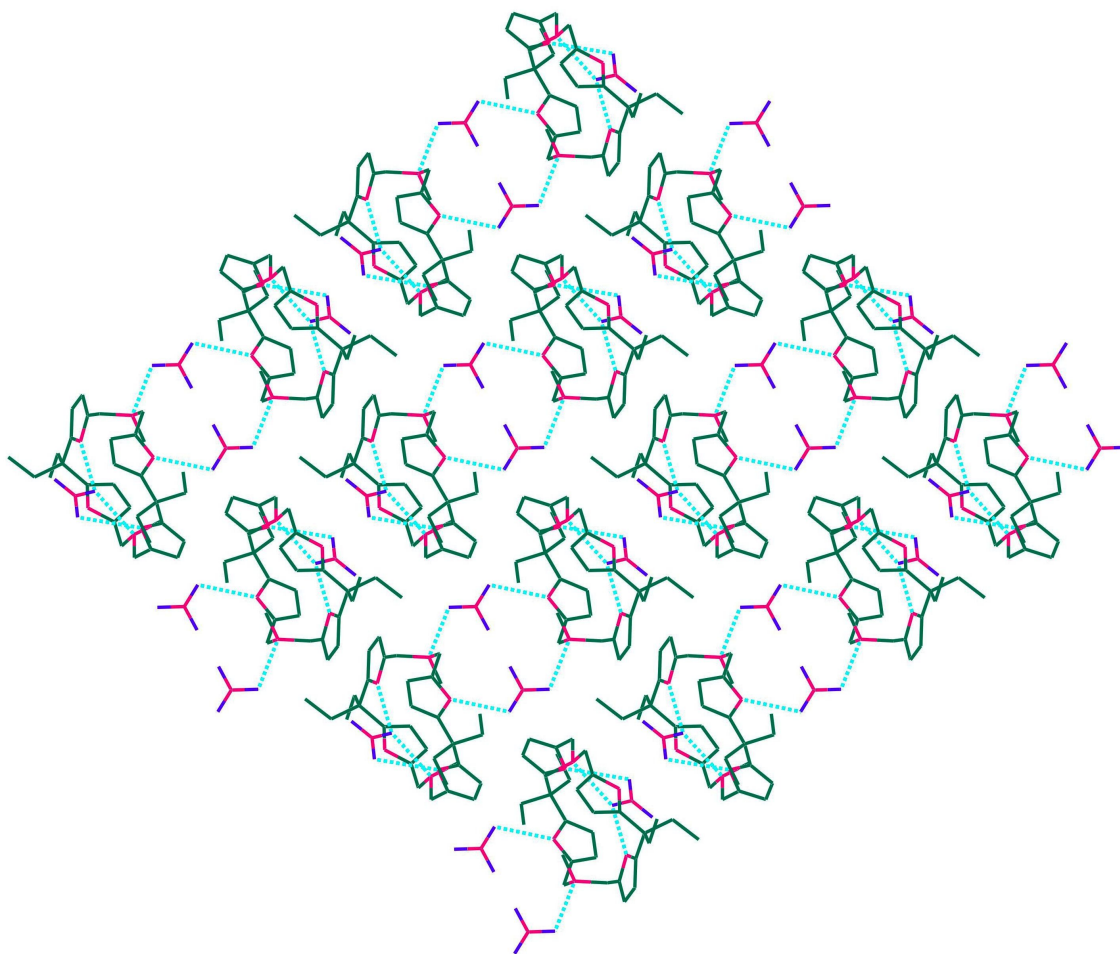


**Figure S23.** 2D diagram of the nitrate ion complex **2a**, showing the crystal packing pattern and interactions viewed along the b axis.

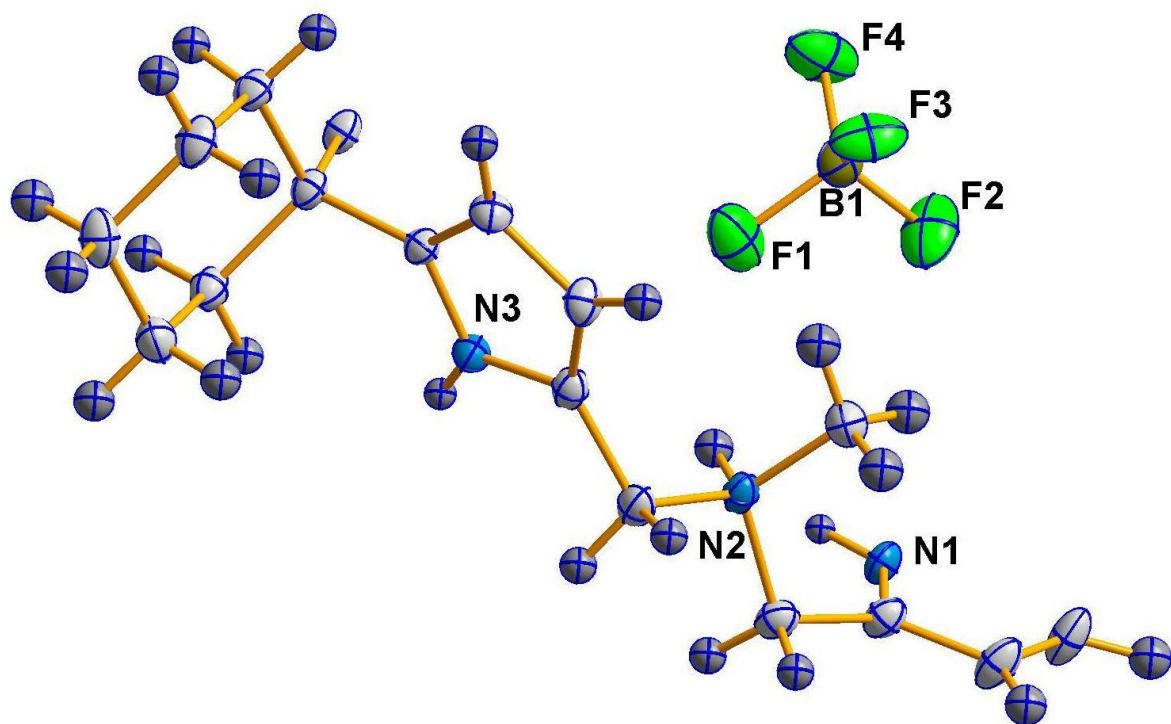


**Figure S24.** ORTEP diagram of the tetrafluoroborate ion complex **2b**, showing the asymmetric unit (50% thermal ellipsoids).

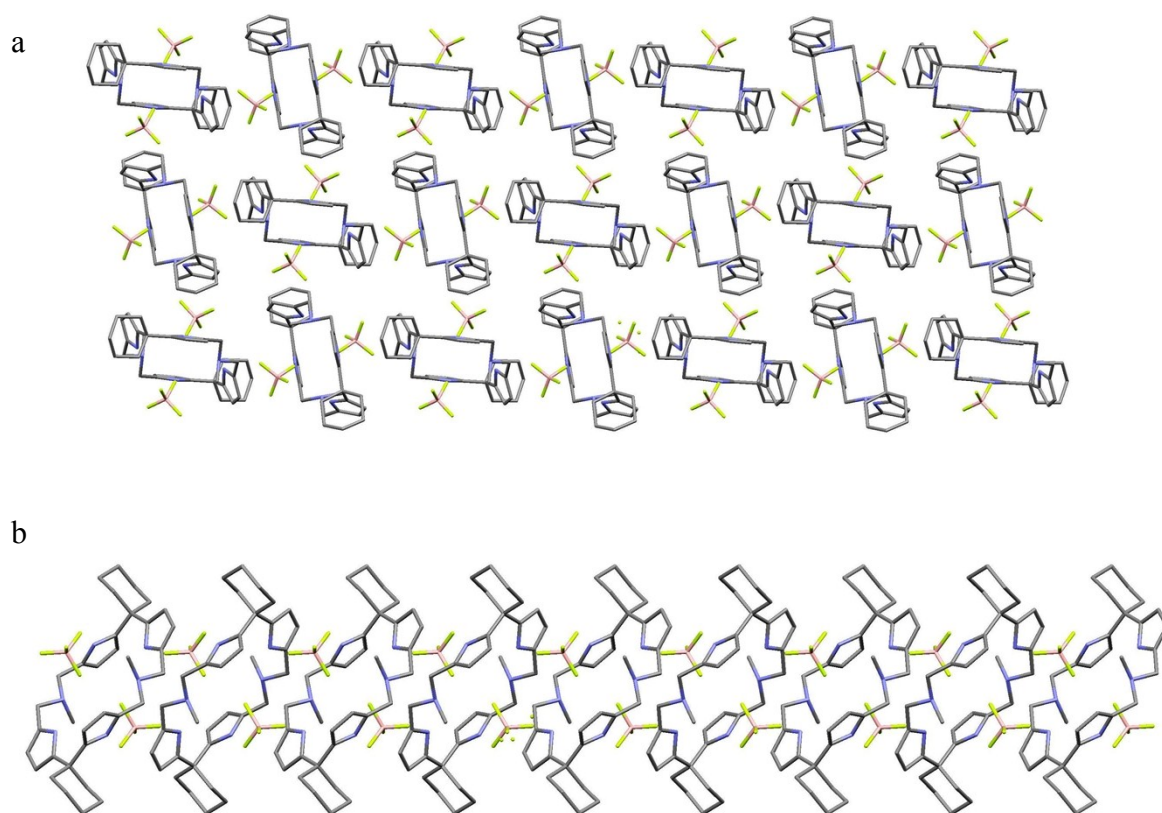


**Figure S25.** (a) 2D packing diagram of the tetrafluoroborate ion complex **2b**, showing the arrangements of the receptors and  $\text{BF}_4^-$  ions. (b) Packing of **2b** viewed along the b axis.

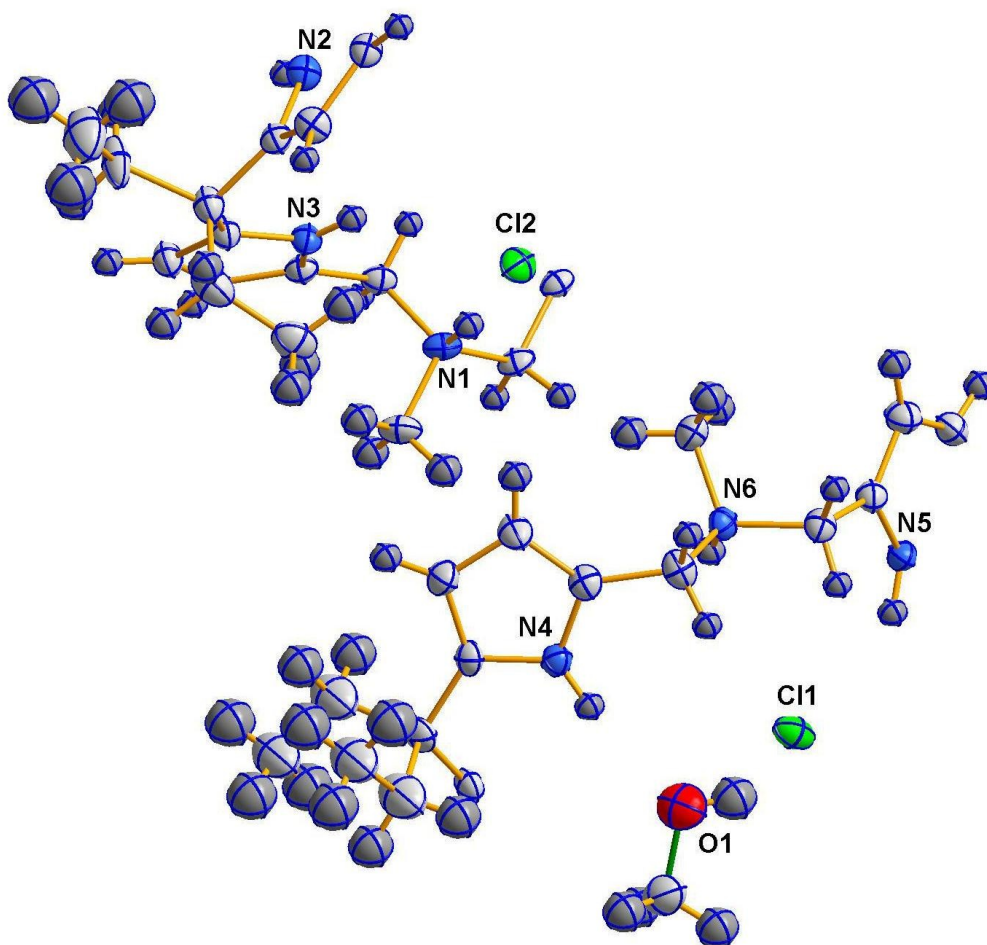


**Figure S26.** ORTEP diagram of the chloride ion complex  $2c \cdot \text{CH}_3\text{OH}$ , showing the asymmetric unit (50% thermal ellipsoids).

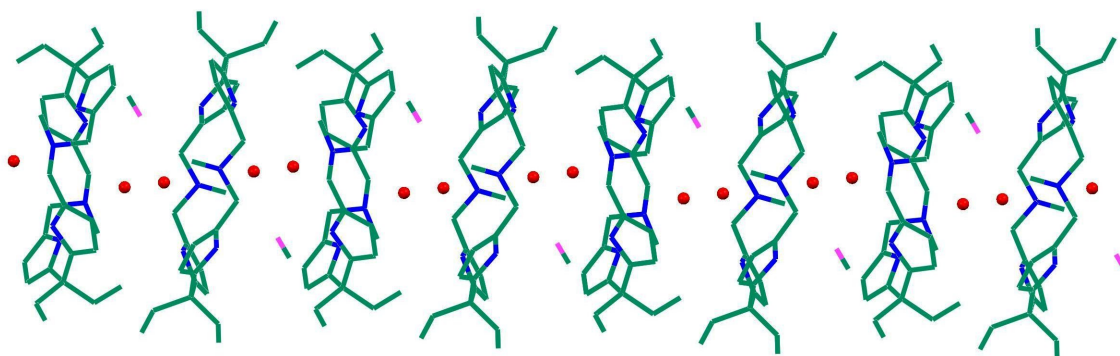


**Figure S27.** 2D packing diagram of the chloride ion complex  $2c \cdot \text{CH}_3\text{OH}$ , showing the alternating arrangements of two different 1,2-*alternate* conformational isomers in the crystal packing viewed along *b* axis.

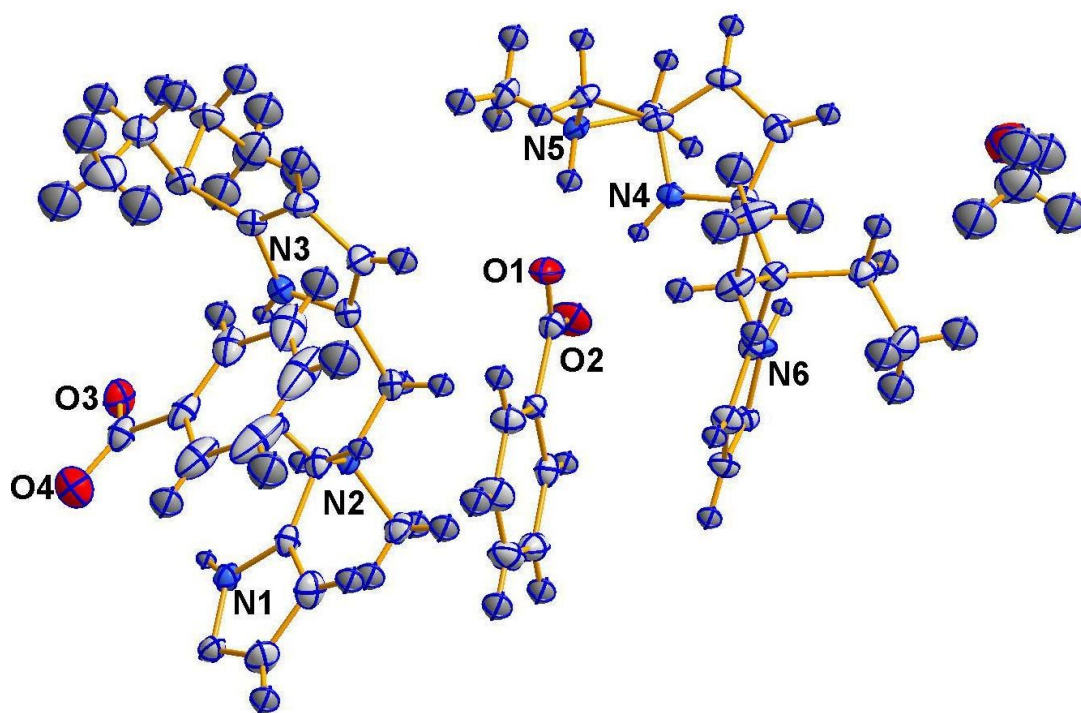


**Figure S28.** ORTEP diagram of the benzoate anion complex **2d**·0.5MeOH, showing the asymmetric unit (50% thermal ellipsoids).

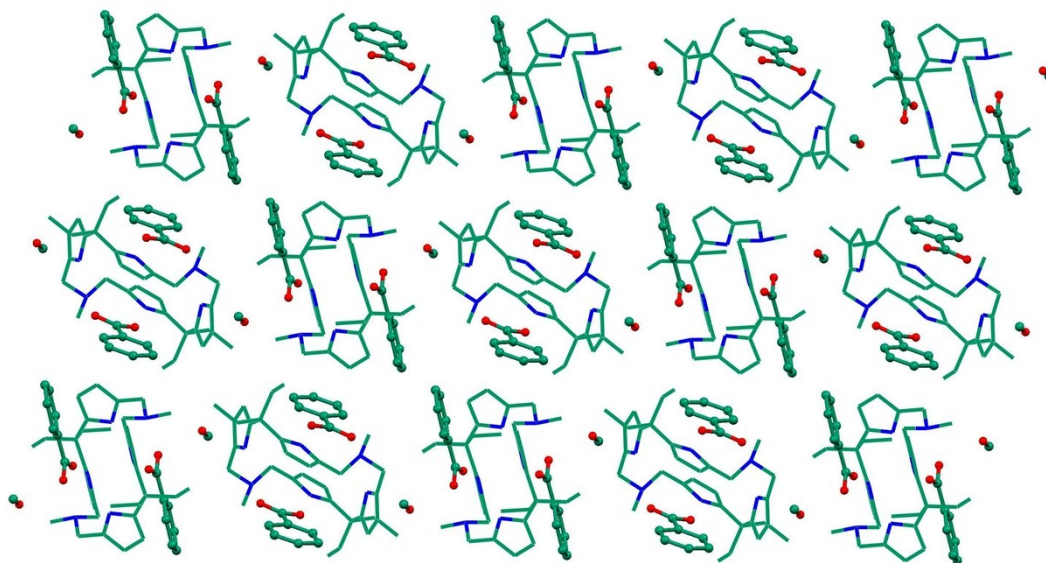


**Figure S29.** 2D packing diagram of the benzoate anion complex **2d**·0.5MeOH, showing the arrangements of the receptors, benzoate anions and methanol solvents of crystallisation.

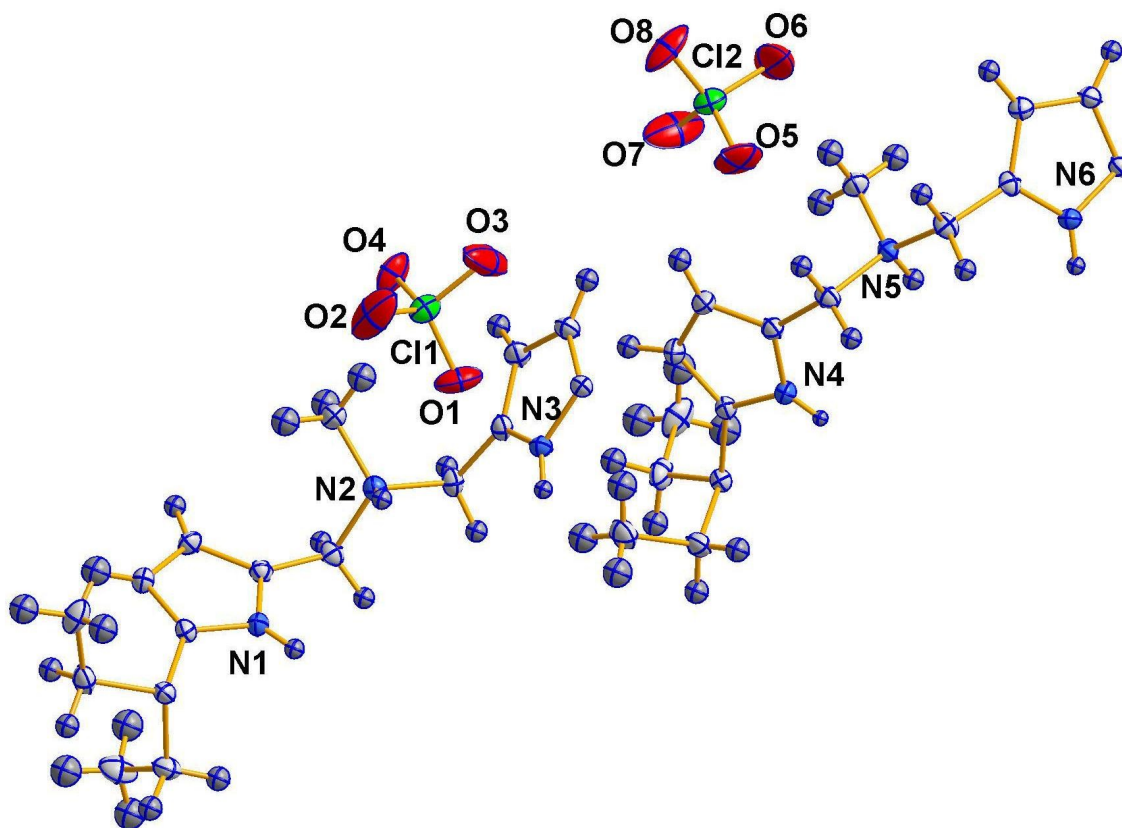


**Figure S30.** ORTEP diagram of the perchlorate anion complex **2e**, showing the asymmetric unit (50% thermal ellipsoids).

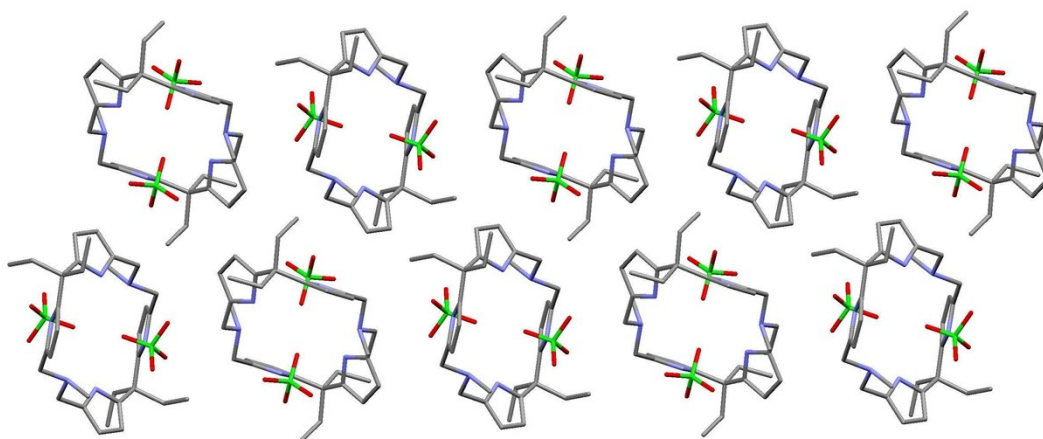


**Figure S31.** 2D packing diagram of the perchlorate anion complex **2e**, showing the arrangements of the receptors and perchlorate anions along a axis.

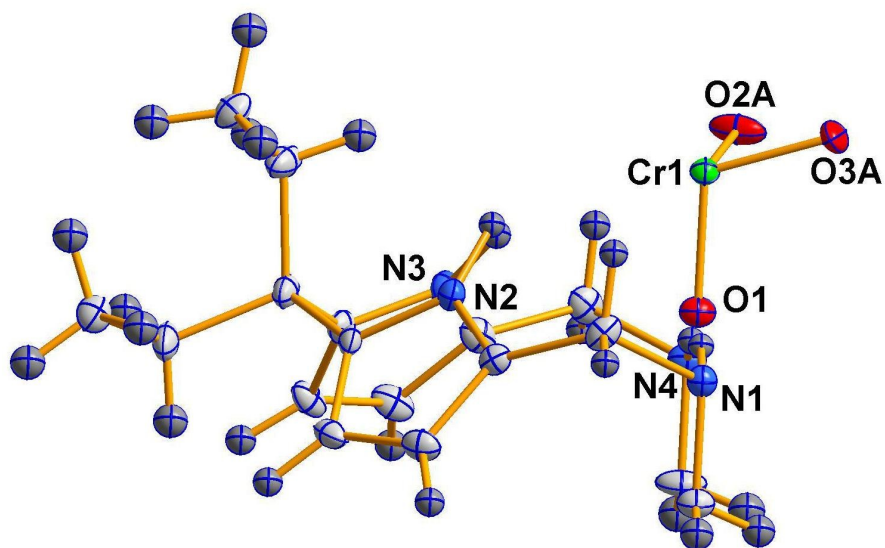


**Figure S32.** ORTEP diagram of the chromate ion complex **2f**, showing the asymmetric unit (50% thermal ellipsoids).

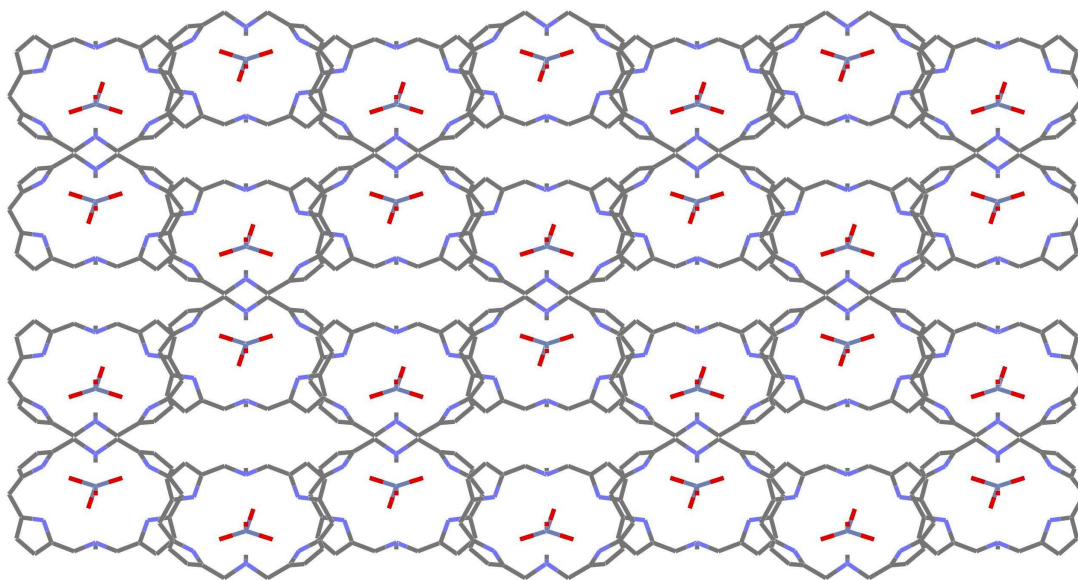


**Figure S33.** 2D packing diagram of the chromate ion complex **2f**, showing the arrangements of the receptors and chromate anions viewed along the c axis.

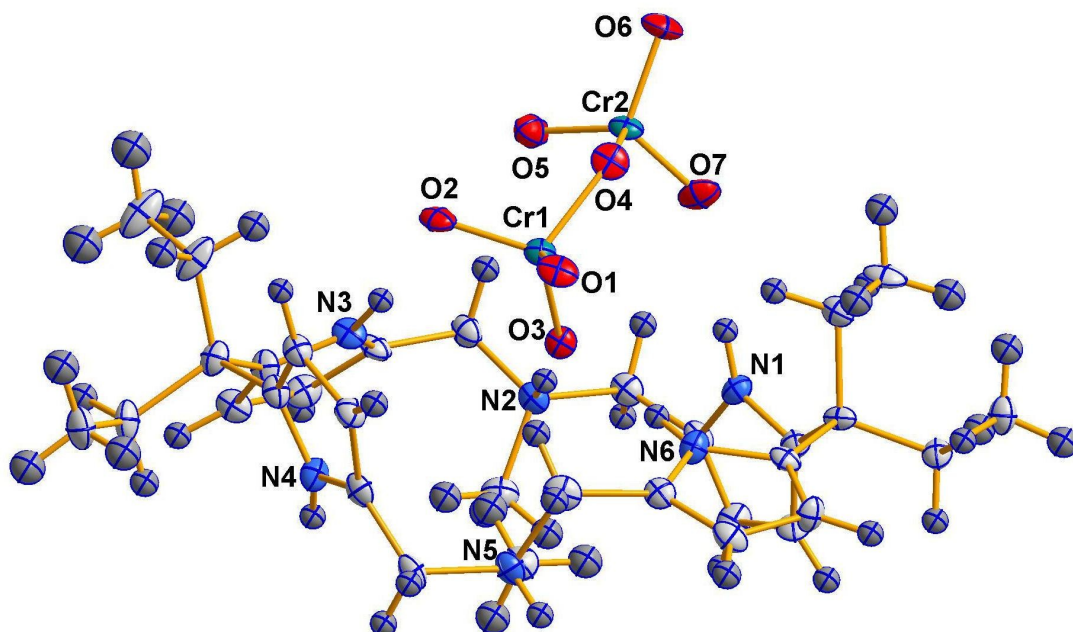


**Figure S34.** ORTEP diagram of the dichromate anion complex **2g**, showing the asymmetric unit (50% thermal ellipsoids).

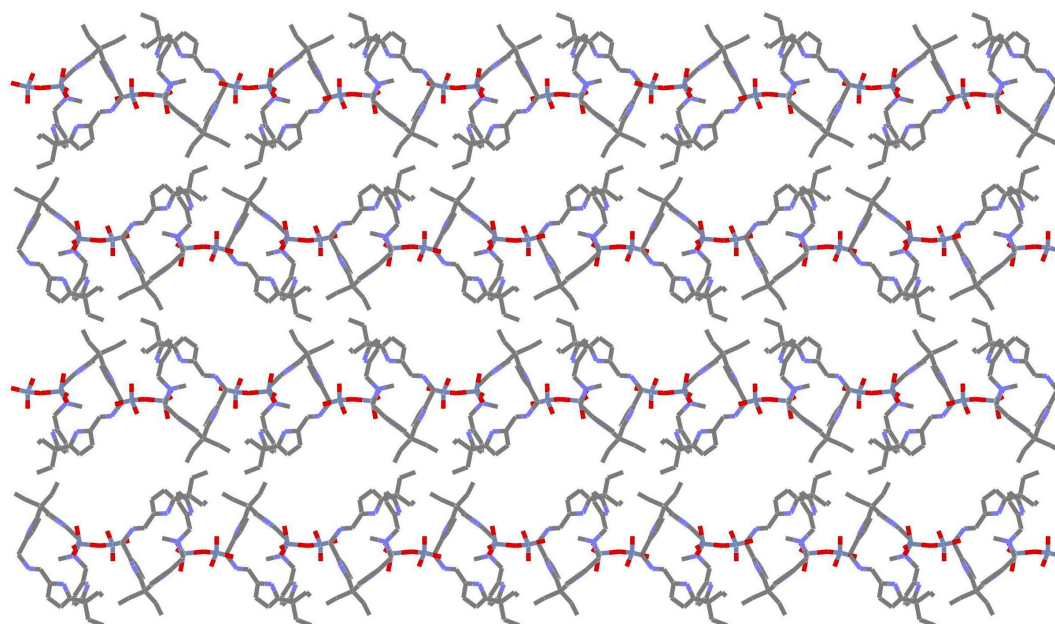


**Figure S35.** 2D packing diagram of **2g**, showing the arrangements of the receptors and dichromate anions viewed along the *a* axis.

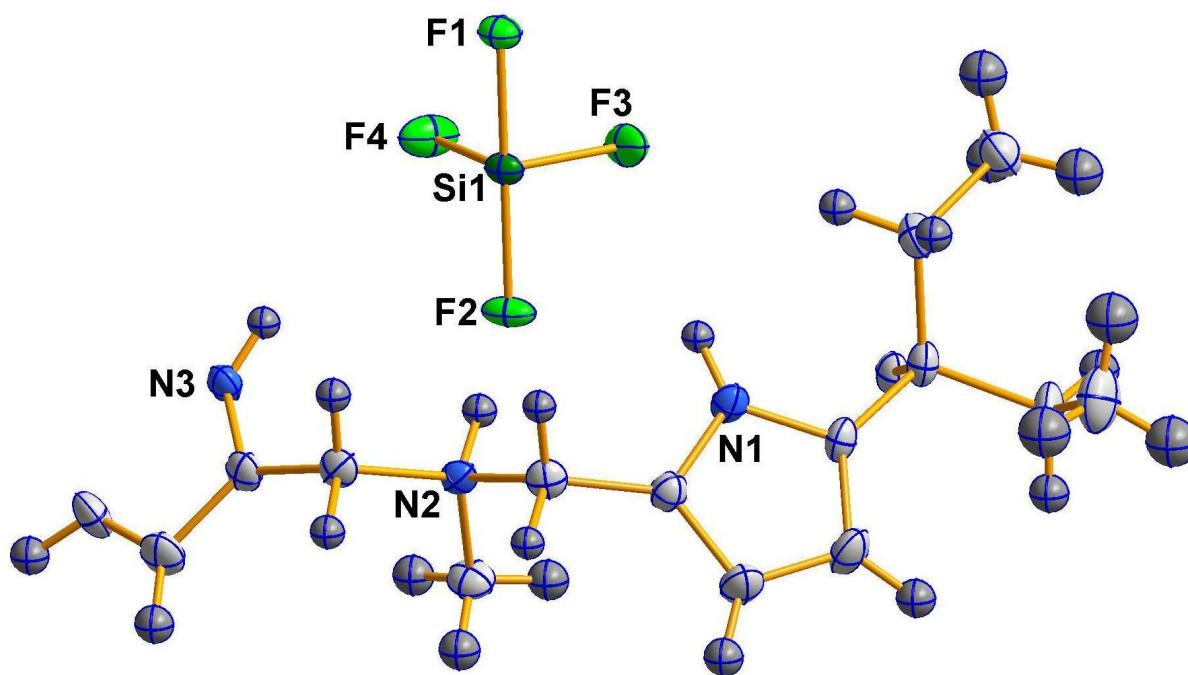


**Figure S36.** ORTEP diagram of the hexafluorosilicate anion complex **2h**, showing the asymmetric unit (50% thermal ellipsoids).

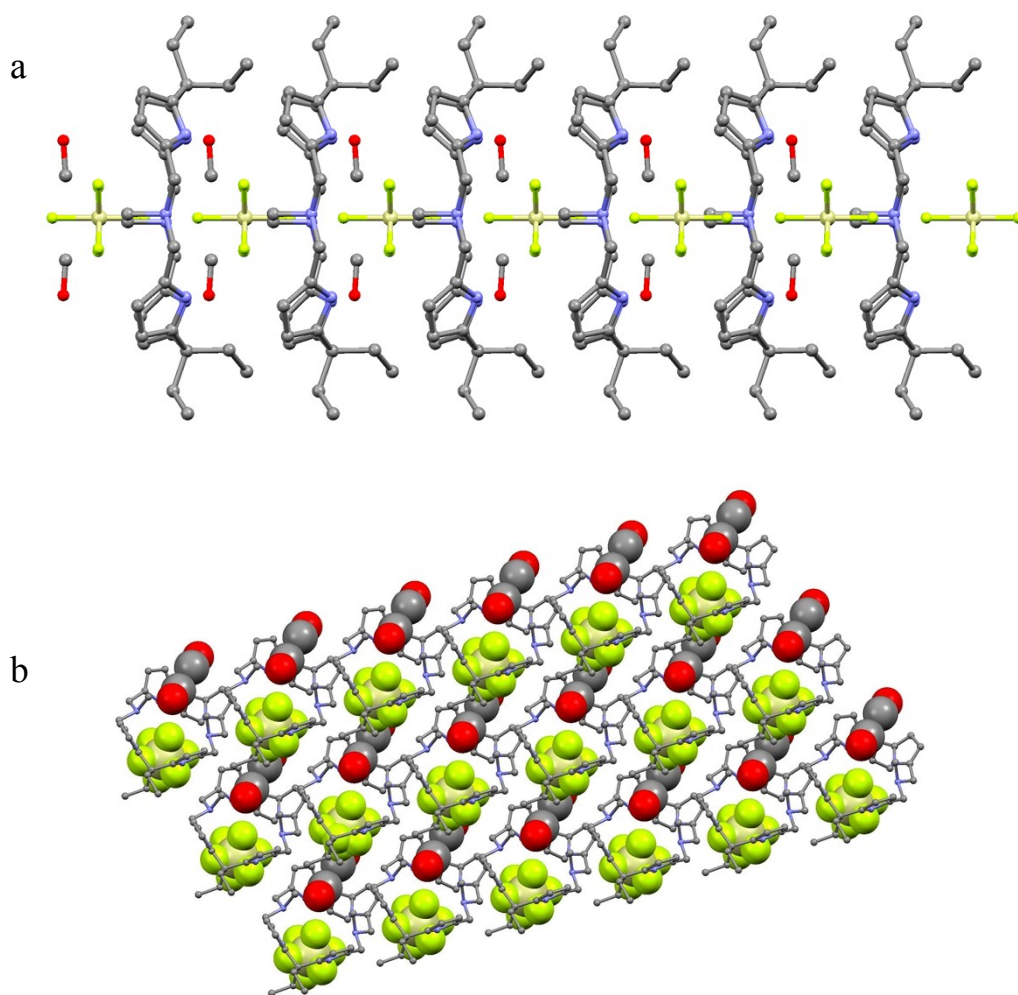


**Figure S37.** (a) 2D packing diagram of **2h**, showing the arrangements of the receptors and hexafluorosilicate anions viewed along the a axis; (b) another view of the crystal packing exhibited by complex **2h**.

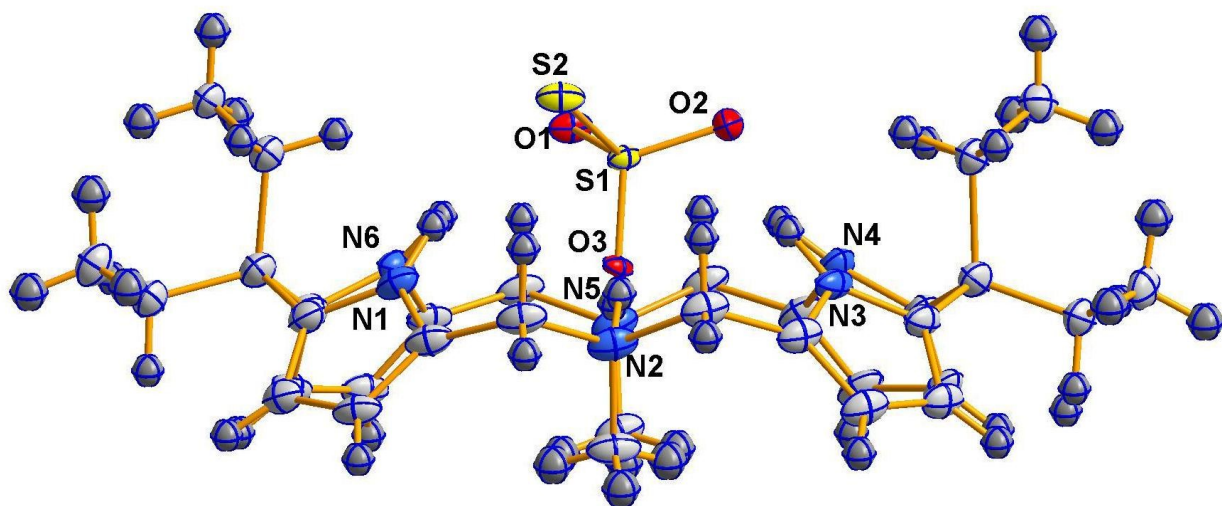


**Figure S38.** ORTEP diagram of the thiosulfate anion complex **2i**, showing the asymmetric unit (50% thermal ellipsoids).

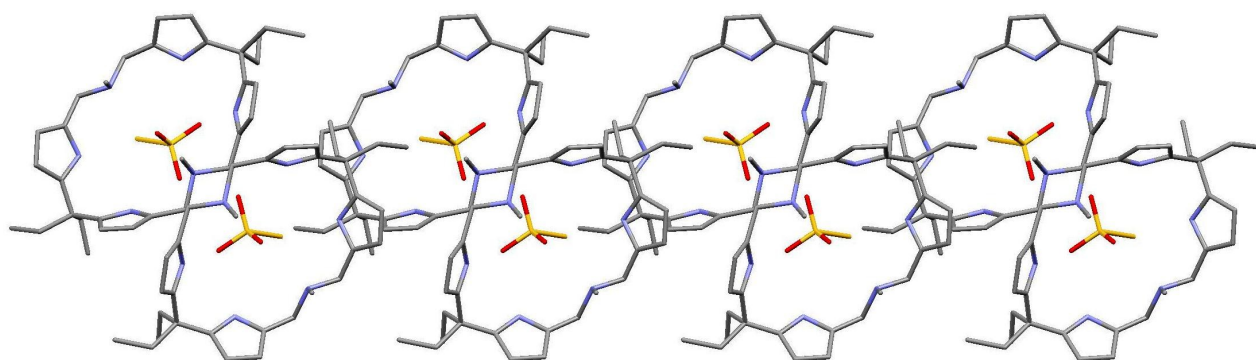


**Figure S39.** 2D packing diagram of **2i**, showing the arrangements of the receptors and thiosulfate anions viewed along the b axis.